

Master's Programme in mechanical engineering

# Pneumatic Energy Saving Unit in Pneumatic systems

Effect of a pneumatic air recirculating unit on energy consumption and on actuator's velocity in a pneumatic system

---

**Lorenzo Ceppari**

Copyright ©2022 Lorenzo Ceppari

---

<b>Author</b>	Lorenzo Ceppari	
<b>Title of thesis</b>	Pneumatic Energy Saving Unit in Pneumatic systems	
<b>Programme</b>	mechanical engineering	
<b>Major</b>	automation	
<b>Thesis supervisor</b>	prof. Petri Kuosmanen	
<b>Thesis advisor(s)</b>	Jyrki Kajaste	
<b>Date</b>	<b>Number of pages</b>	<b>Language</b>
11/07/2022	67 + 11	English

---

**Abstract**

It has been estimated that around 10% of the total industrial electricity power consumption in the EU can be attributed to compressed air systems. pneumatic system's efficiency usually is between 10% to 30%. An increase of 15 to 30 % in energy efficiency would correspond to \$1.5 billion annual savings. PESU, Pneumatic Energy Saving Unit supplies repressurize actuator's exhaust air back in the pneumatic system. Three pneumatic systems were built and tested. Gathered data were analyzed. The effects of PESU on pneumatic systems were analyzed. Power consumption and cycle time comparison were done.

PESU was found to decrease energy consumption between 37% to 39%, while actuators' cycle time increased between 10% to 24%. PESU is then considered a valuable investment in industry only where its application does not slow production rates.

---

**Keywords** Compressed air, mass flow rates, cycle time, productivity

---

# Contents

Preface.....	vi
Introduction.....	3
1.1 Main sources of power losses.....	4
1.2 Application of pneumatics in industry .....	5
1.3 Other research paper done on this topic .....	6
1.4 Introduction to this thesis topic.....	6
2 Introduction to PESU.....	8
3 Development of the test system .....	11
3.1 Test 0's system .....	11
3.1.1 Description of the first test system .....	11
3.1.2 Oil and moisture filters .....	12
3.1.3 Sensors.....	13
3.1.4 Flow meter valve.....	13
3.1.5 Actuators.....	14
3.1.6 Other components.....	15
3.2 Test 1's system .....	16
3.3 Test 2's system.....	17
3.3.1 Magnetic gripper .....	19
3.4 Test 3's system.....	19
3.5 External power supply .....	19
4 Tests system description .....	20
4.1 Terminal wiring.....	20
4.2 Pneumatic system .....	21
5 Control algorithm.....	23
5.1 Test 0's control algorithm .....	24
5.2 Test 1's control algorithm.....	25
5.2.1 Position sensors.....	25
5.3 Test 2's control algorithm .....	28
5.3.1 Test 2 movement description.....	29
5.4 Test 3's control algorithm .....	29
6 Tests.....	31

6.1	Test 0 test procedure.....	31
6.2	Test 1, 2 & 3 recording procedure .....	32
6.3	Checking mass flow rates .....	32
6.4	Checking pressure drops .....	37
7	Results .....	45
7.1	Total energy consumption .....	45
7.2	Time cycles .....	46
7.3	Energy consumption per cycle.....	46
7.4	Data results.....	47
8	Results analysis .....	48
8.1	Mass flow rates behavior.....	48
8.2	Pressure in the actuators.....	50
8.3	Pressure values before at the supply and at the exhaust.....	53
8.4	Causes of speed reduction.....	55
8.5	Sudden rises in flow rate when the unit is applied.....	57
8.6	Supplied pressure value .....	59
8.7	Temperature changes.....	60
9	Data analysis.....	62
9.1	Performances analysis.....	62
9.2	Return on investment period analysis.....	63
10	Conclusion .....	65
10.1	PESU speed reduction.....	65
10.2	Possible future tests .....	65
10.3	Economic liability of PESU.....	65
10.4	Issue with gathered data.....	66
11	Bibliography .....	67
	Appendix A.....	71

## **Preface**

I want to thank university teacher Jyrki Kajaste for it is involvement in the project in the figure of instructor, Professor Kuosmanen Petri as the role of supervisor professor, research engineer Sinkkonen Antti for all the time that he took time my to answer to my question about technical equipment. To Kim Hirvonen, Anna-Kaisa Korhonen and Oliver Olin and the work that we did together during MEC-E5002 Mechatronics project. A more general thanks goes to all the staff working at Aalto's hydraulics lab.

I also want to thank my girlfriend Svenja for keeping me sane and alive.

I thank my mother for having supported and financed me in my choice. My sister for showing me the way when I couldn't see it.

Otaniemi, 11 July 2022

Lorenzo Ceppari

## Abbreviations and Acronyms

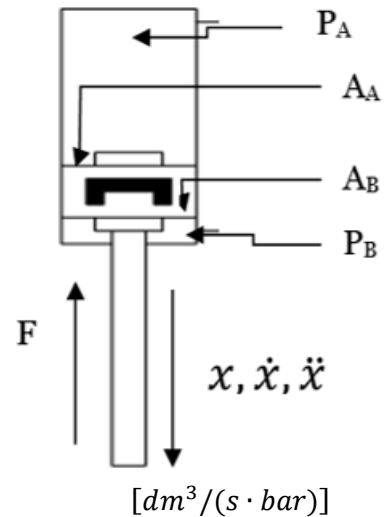
CA	Compressed air
PESU	Pneumatic energy saving unit
CAS	Compressed air system
FS	Full scale value of a sensor
90 <sub>fit</sub>	90° pneumatic fitting
3 <sub>way,fit</sub>	3-way port pneumatic fitting
Act <sub>1</sub>	Actuator 1
DCV	directional control valve

## Definitions

experiment	Same circuit tested with and without PESU
test	Different circuit with different actuators

## Symbols

$\dot{m}$	Mass flow rate	[kg/s]
$m$	Total amount of consumed CA	[kg]
$Q$	Volumetric flow rate	[m <sup>3</sup> /s]
$A$	Piston area	[m <sup>2</sup> ]
$\rho$	Air density	[kg/m <sup>3</sup> ]
$P$	Air pressure	[bar]
$R$	Air gas constant	[J/(kg K)]
$T$	Air temperature	[°C]
$F$	Force	[N]
$x$	Actuator's position	[m]
$\dot{x}$	Actuator's velocity	[m/s]
$\ddot{x}$	Actuator's acceleration	[m/s <sup>2</sup> ]
$e$	Error	[-]
$C$	Sonic conductance	[dm <sup>3</sup> /(s · bar)]
$B$	Critical pressure ratio	[-]
$P_1$	Upstream pressure	[MPa]
$P_2$	Downstream pressure	[MPa]
$P_{cr}$	Critical pressure	[MPa]
$F_v$	Friction forces in actuator movement	[N]
$F_{ext}$	External forces (gravity load, external load, ...) applied on the actuator	[N]
$H(s)$	Sensor's delay Laplace transform	[-]
$U(s)$	Physical signal Laplace transform	[-]
$Y(s)$	Sensor's analog signal	[-]
$t$	time	[s]
$W_{in}$	Input power	[W]
$E_{in}$	Total input energy	[J]
$\Delta profit$	Difference between profit	[€]
$U$	Initial investment regarding applying the unit	[€]
$i$	Interest rate	[-]
$n$	Number of years to pay back the initial investment	[-]
$T_0$	Temperature at standard condition	[K]
$P_0$	Pressure at standard condition	[Bar]
$\rho_0$	Fluid density at standard condition	[kg/m <sup>3</sup> ]



## Introduction

Development in computational power in the last decades gave birth to ever increasing sophisticated microcontroller. This, along with the development of smaller, efficient, and more reliable sensors opened the doors to the development of automation. Automation has been present in industrial production for over forty years, but not all sectors or companies are affected by it. The development of automation in enterprises, where it is present, and the application of it in sectors, where it is not present, will most likely cause economic growth as well as better life conditions.

With automation many problems arise, also. Neglecting social issues that arise from losses of job places. Automating industrial process, machines need to be powered. It is well known that industry mostly rely on CO<sub>2</sub> emission power sources(1). Climate changes awareness, recent increase in costs of energy production and the need for companies to remain competitive on the market forces industry to find new methods to reduce energy consumption.

In automation machines are actuated by three kind of energy supply: electrical actuators, hydraulic actuators, and pneumatic actuators. All of these have different pros and cons. In application where load is relatively low, and speed is required pneumatic actuators are preferred.

Pneumatics uses pressurized air as a working fluid. With the respect to the other drivers, electricity and hydraulics, pneumatics is the cheapest and safest to use.

In pneumatics if the system is leaking, risks would be lower than if a hydraulic system is leaking. Air is a harmless fluid, volatile and can be easily disposed to the atmosphere. Hydraulic fluids (mostly mineral oils) used in the industry are toxic, when leaking they contaminate the surrounding area. It is not easy to get rid of an cannot be disposed in the environment.

With the respect to electrical drivers, pneumatics is usually cheaper. Substituting an electrical component, for instance a servomotor, can be very expensive.

Then, if pneumatic components are so great, why they represent only a small fraction total actuators present in industry?

The main reason is operational costs related to pneumatics. Compressed air system (C.A.S.) have low efficiency. Usually pneumatic system efficiency is between 10% to 30% (2). Typically in CASs costs related to energy consumption represents the 75% of the total cost, while 12% is the initial investment and 13% is maintenance (2).

Nevertheless, pneumatic systems are widespread in industry. It has been estimated that around 10% of the total industrial electricity power consumption in the EU can be attributed to compressed air systems (3).

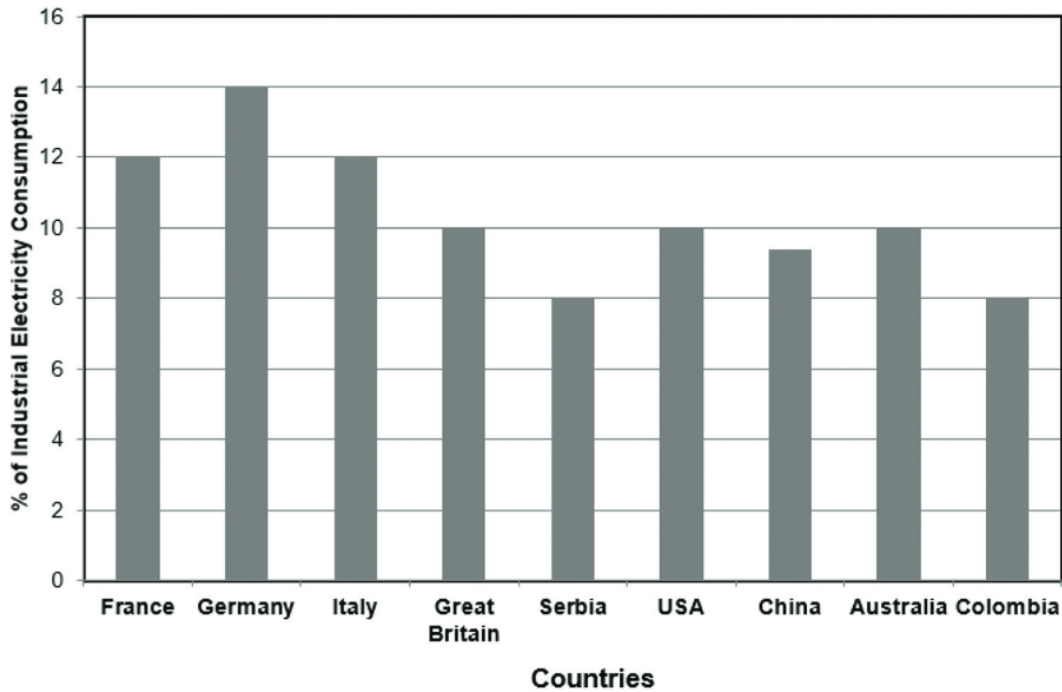


Figure 1: Power consumption per country (2).

In the U.S.A. pneumatic equipment consumes roughly 530 PJ of energy annually, which correlates to \$10 billion worth of energy per year. An increase of 15 to 30 % in energy efficiency would correspond to \$1.5 billion annual savings (4).

Pneumatic systems have such low efficiency for several reason: leakages, unproper hosing, uncontrolled system parameters, and wrong compressor's working conditions are the main ones (5).

## 1.1 Main sources of power losses

Most commonly lack of knowledge on CAS behavior is source of important power losses. As (5) states: "the actual state of the CAS within the Italian industry shows an average-low qualitative level either for dimensional, operational and managerial functions". Leakages are a major power loss in CASs. Abela (6) showed how leakages from a 1.5 mm diameter hole in a 6 bars system could cause losses of a 755 € per year or the amount of energy produced by ten photovoltaic panels in a year. A study conducted in a Bulgarian bottling factory (7) found more than a thousand meaningful leakages (higher than 5 L/min). Often leakages are the main reason behind the mis-

conception that pneumatic system are inefficient by nature. A study conducted by FESTO in 2013 (8) estimated that the surveyed CAS could save more than €7000 per year. Additionally, a greater usage of air, means greater compressor performance, shorting life cycles and increasing costs.

Two very popular methods exist to evaluate leakages in CASs, both of which are non-destructive tests. One is using acoustic sensors. Leakages from small diameter holes generate sounds waves too high in frequency to be heard by human ear. Thanks to specific microphone, sound waves ranging from 20 kHz to 100 kHz can be detected. For flexible hoses ultrasound detection should be used when emitted leak's sound waves are lower than 74 dB (because background noise interferes with readings) i.e., for leakage holes smaller than 1.3-2.0 mm. For steel pipes ultrasound detection cannot be used since leakages' sound wave exceeds the 74 dB threshold.

A more reliable method to evaluate leakages from bigger leaks is infrared thermography (IR). When air leaks from holes its temperature increases. Thermal vision cameras detect infrared waves generated by the heated leaking air. IR is not suitable for small holes; temperature gradient is too small. IR is sensible to environment and extreme lighting conditions (9).

It was also shown in different papers (5) that, a low amount of industrial CASs have monitored system variables. A monitored system can be controlled, and air supply could be turn off when needed. If a system is not monitored, no control can be implemented.

Misconception about pneumatics' low efficiency is largely due to an unproper use of CASs. Leakages are very hard to avoid but a reduction in the number of leakages and preventive maintenance will reduce the costs of CASs.

## **1.2 Application of pneumatics in industry**

Thanks to their characteristics, CASs are most suitable in applications with low load and where speed is required. Pick and place, which requires fast movement and does not usually involve moving heavy components, is one of the applications where pneumatics is commonly used.

As an example, in automated production lines, products are usually either machined or assembled in different stations. When a semifinished product leaves a station, it must be move to the next station. To maximize productivity pick and place operation must be as fast as possible. Also, according to what product is being produced, moved products are not very heavy.

In pneumatics different type of actuators exists single acting piston, double acting piston, rotary actuators, rod-less actuators.... they all have different

characteristics and purpose. The most common pneumatic actuators used in pick and place operations are grippers, which are a family of actuators, which can gasp onto products. These actuators are easy to use, effective and reliable.

### **1.3 Other research paper done on this topic**

Many authors have proposed other methods to increase pneumatic efficiency.

In 2013 Blagojevic (10) analyzed the effect of recirculating exhaust air via a servo valve. Along with the experiment, a control algorithm was developed to reduce air consumption by actuating the recirculating exhaust servo valve. Results achieved a reduction of 29.5% air consumption. More recently Blagojevic (11) suggested a servo mechanism which is able to clamp the piston at the movement end in order to minimize supply pressure level, thus reducing the amount of supplied air. Unfortunately, this setup proven to be a valuable investment only for small actuators

Another of the effect of recirculating exhaust air in pneumatic actuators was conducted in the work by Cummins (12) in which exhaust air was stored in a pneumatic strain accumulator. Results showed an efficiency increase between 32% to 78%.

### **1.4 Introduction to this thesis topic**

In traditional applications, pneumatic exhaust air from actuators is released into the atmosphere. Exhaust air has higher pressure than the one of the atmosphere. This results in a waste of power.

A patent from 2017 (13) focused on recirculating exhaust air via a pneumatic energy efficiency unit (PESU) to the actuator supply.

PESU is a mechanical unit. It does not need any power input or servocontrol. The unit is supplied with two flow rates, one coming from the supply and one from the actuator's exhaust air. Two outlets are present, one directs air flow to the actuators, the other releases air flow to the environment.

The unit contains several pneumatic components. Air is recirculated through a pneumatic booster. A series of poppet valves are used to avoid backflow. The working principle of PESU is addressed in chapter 2.

The unit has already proven to be effective. Tests done by the Finnish company owning the patent, bf+ energia and during Aalto university's mechanics project course MEC-E5002 showed a reduction in compressed air (C.A.) consumptions.

In this thesis the effects related to the application of P.E.S.U. were studied. Experiments were undertaken with a different approach than the one done in MEC-E5002.

To test the system, the one system developed in MEC-E5002 was used. At first, improvement to its design were done. Then a test procedure was decided, and a control algorithm was implemented. Results were then analyzed.

The main goal of the experiments was to evaluate if the application of PESU in an industrial CAS is a valuable investment. PESU energy reduction and actuators' cycle time increase were estimated. Then an economic analysis was done.

## 2 Introduction to PESU

In *Figure 2* the schematics of PESU is shown according to patent US9765786.

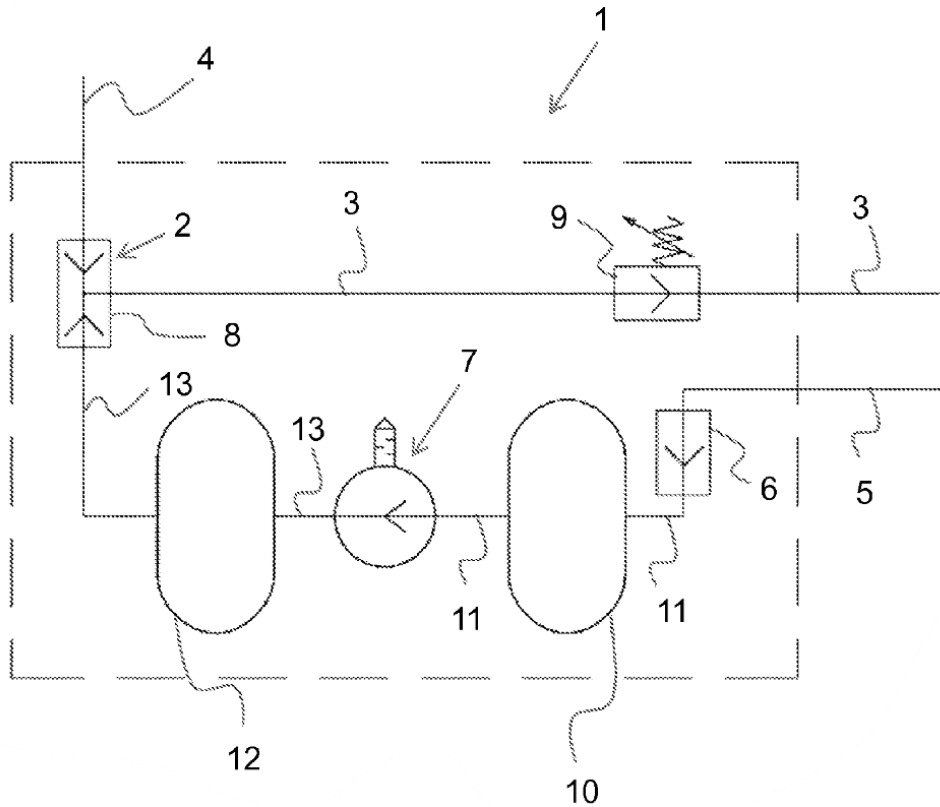


*Figure 2: PESU schematics.*

The patent shows four different set ups, the provided model is depicted in figure 1 of (13).

Air is supplied to unit **1** through pipeline **4** from an external main source (such one or more compressors). CA is conveyed through pipeline **3** to the application. The first receiving means **2** is arranged to receive and guide CA to pipeline **3**.

Reduced-pressure air that was utilized by the application is recovered in the unit by means of pipeline **5**. Along pipeline **5** a second receiving unit **6** (preferably comprising of a non-return valve) allows flow to enter the unit **1**. Pipeline **11** is then supplied with reduced-pressure air.

Recycling reduced-pressure air requires that application's exhaust air's pressure value is increased. This is solved by pressure intensifier **7** (or pressure booster) connected to a check valve. By utilizing energy contained in the gas flow, air's pressure is increased.

Re-pressurized air, having higher pressure values than before, is now present in pipeline **13** and is lead to a substitution means **8** (e.g., a shuttle

valve) placed between **3** and **4** (In its preferred embodiment, **8** is included in **2**). When recirculated air from **13** reaches higher pressure values than pressure values from **4** (main supply), **8** allows flow to **3** while **2** cuts off flow from main supply.

Pipeline **3** may also be provided with a pressure controller **9** to adjust re-pressurized air's pressure to match pressure values from the main supply. By providing the unit **1** with a first tank **10**, it is possible to store reduced-pressure air for the treatment. The pressure-increasing unit **7** may also be provided with a second storage tank **12**, interconnecting **7** with **8**, to store air until re-pressurized air has not reached higher pressure values than supply pressure.

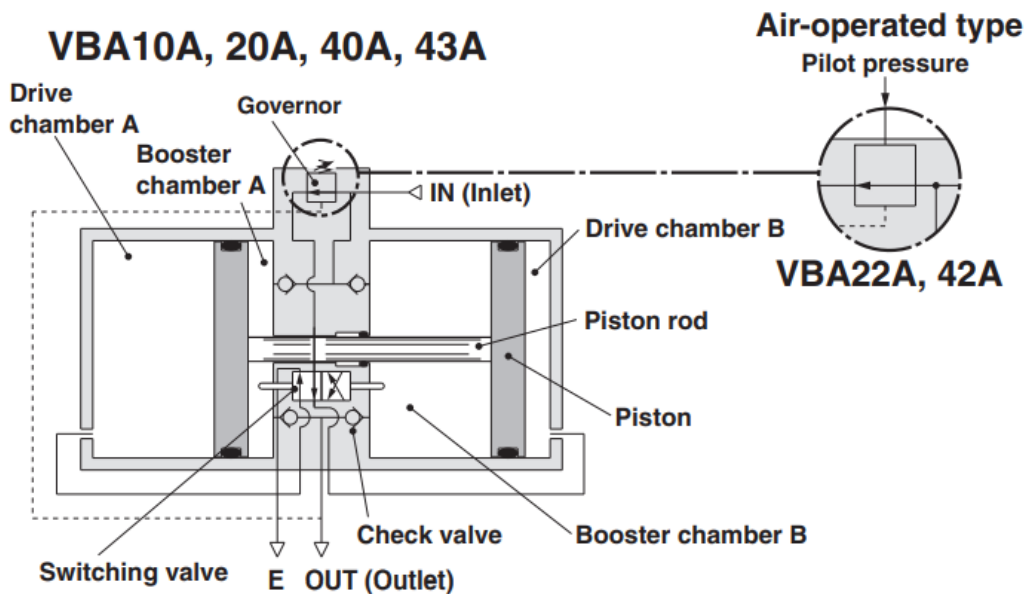


Figure 3: Pneumatic pressure booster schematics.

The cited patent's main component is the pressure booster **7**. A pressure booster can be described as two double acting piston. There are many variations of pneumatic booster. Its working principle is similar for every model and is here described as reported on SMC® pressure intensifier catalogue (14). "The **IN** air passes through the check valve to **booster chambers A and B**. Meanwhile, air is supplied to **drive chamber B** via the governor and the switching valve." Now **drive chamber B, booster chambers A and B** contain the same pressure value (equal to **IN**), while **drive chamber A** pressure value is equal to the one of the exhaust. Pressure difference between **booster chamber A** and **drive chamber A** moves the piston towards the left side "boosting the air in **booster chamber B**. As the piston travels, the boosted air is pushed via the check valve to the **OUT** side." Once the piston reaches the end stroke, the piston, via mechanical contact, causes the switching valve to change its position. This way the switching valve is found in the opposite configuration. Now "drive **chamber B** is in

the exhaust state and **drive chamber A** is in the supply state respectively.” At the end of the stroke, pressure values in **booster chamber A and B** are equal to the one in **IN**. “Then, the piston reverses its movement, this time, the pressures from **booster chamber B** and **drive chamber A** boosts the air in **booster chamber A** and sends it to the **OUT** side. The process described above is repeated to continuously supply highly pressurized air from the **IN** to the **OUT** side. The governor establishes the outlet pressure by handle operation and pressure adjustment in the drive chamber by feeding back the outlet pressure.”

The provided PESU model contained a pneumatic booster from SMC®. The unit was pre-set, and no additional modifications were done on the booster or on the circuit.

The only setting done by the user was to regulate component **9** (which handler is the only component visible outside the unit). This setting was required by the user manual (15). Component **9** was set to its maximum pressure level to analyze the effect of PESU when the unit had no restriction. Additionally, the provided PESU model lacked component **10** (reduced pressure tank). The only present tank was component **12** (re-pressurized pressure tank).



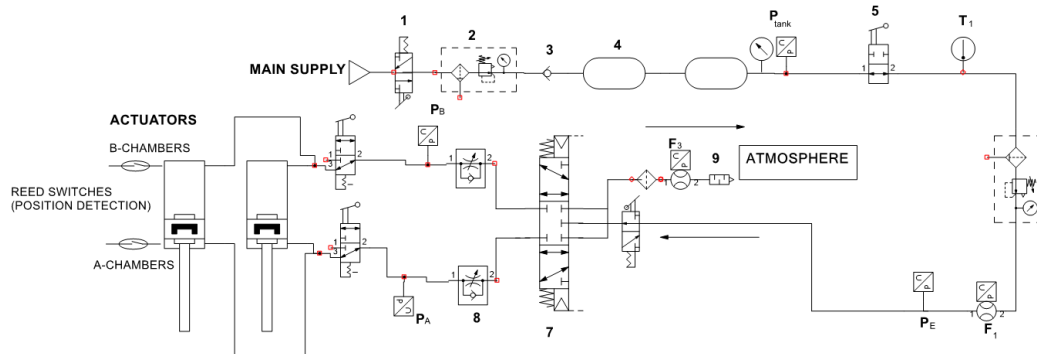


Figure 5: Schematics of the system without P.E.S unit.

The system had a very simple design: one supply, pressure tanks to store air, PESU, and a directional control valve to change the actuator direction. To be able to insert flow and pressure sensor air quality had to be guaranteed. It was then required to insert filter to clear CA from oil and water content. There was also the need to ensure that some parts of the system could be isolated from the rest of the system. This explains the reason why so many components are present in the system. To detect the cylinder's position, one Reed sensor is positioned to each end of the stroke.

A brief description of the components is given in the next subchapters.

### 3.1.2 Oil and moisture filters

The system is supplied with air coming from the hydraulics lab's compressed air supply. Atmospheric air always has some level of moisture in it. The total amount of moisture in air is dependent on pressure and temperature. At higher temperature and pressures the total amount of vapor weight ratio contained in air is higher than at lower temperature and pressure values. When, in conditions of saturated air, if temperature decreases or pressure increases, an amount of moisture condensates into water (16).

When air is pressurized, it is drain from vapor contents. But a small amount of vapor is always present.

In the case of a pneumatic system located inside a university laboratory, external temperature changes are negligible. The amount of moisture is dependent on the changes of pressure values.

When air undergoes transformation, according to state variables values and moisture content, some water may condensate. This could damage components.

Also, air vapor content releases ions which causes corrosion.

Many components are sensible to corrosion. A dryer must be always present at the inlet of a pneumatic system.

It is common practice to insert oil droplets in a pneumatic system (17). This is done to lubricate moving parts. Oil, along with other contaminants, can damage measurement equipment or interfere with the readings. They must be filtered out when compressed air enters the system.

In the system there were inserted four oil filtering units which also helps with removing dirt and one moisture removal unit. The moisture removal unit and an oil filter unit are located at the inlet of the system. It is done to avoid storing oil and moisture in the system.

The other three oil filtering units are situated before every flow metering valve.

### **3.1.3 Sensors**

In test 0 no position sensor was available. It was then chosen to use two reed switches to detect piston position. Reed sensors are magnetic switches, i.e., electrical circuits that, when a magnetic field is detected, close the circuit outputting signal. In this case the piston's base contains a permanent magnet. The sensors can detect the piston's base. If one sensor is positioned at the up-end stroke and one at the bottom-end stroke, the piston position can be detected.

The other detected variables are pressure, temperature, and flow rate. Sensor's codes are reported in the table at page 16.

### **3.1.4 Flow meter valve**

SMC® flow metering sensors need to be fed with the clearest air as possible (18). This is done not to damage the sensor. The working principle of it is very sensible to dirt.

The sensor is composed of some small metal bars inserted in the flow. To measure the flow, the sensor heats itself up. When flow is crossing the sensor bars, the temperature in the metal bars drops down by convection done by the flow rate. According to the cooling rate, the sensor calculates the flow rates. If the metal bars are covered with oil residuals or moisture, the sensor won't cool properly.

Even though fluid filtering induces pressure losses. Flow metering sensors are expensive and thus, air filtering is needed to get reliable results and to protect them.

The sensor outputs the volumetric flow rate in [L/min] at standard conditions. Standard condition corresponds to air at  $T_0=20^{\circ}\text{C} = 293 \text{ K}$  and  $P_0=1 \text{ Bar}$ .

Additionally, the flow sensor outputs signal with a known delay. The sensor's catalogue reports that it takes one second for the sensor to report 90% of the FS value when the sensor is subjected to a step function from 0 to FS value. Knowing this the Laplace transformation values can get derived.

The sensor's output analog signal in Laplace domain  $Y(s) = H(s) \cdot U(s)$  Where  $U(s)$  is the physical signal, while  $H(s)$  is the sensor's delay in Laplace domain.

From catalogue the physical signal is equal to:

$$U(s) = \mathcal{L} \left\{ FS \cdot \begin{cases} 0, & t < 0 \\ 1, & t \geq 0 \end{cases} \right\} (s) = \frac{FS}{s} \quad (1)$$

While sensor's delay Laplace domain is:

$$H(s) = \frac{1}{\tau s + 1} \quad (2)$$

Then:

$$Y(s) = H(s) \cdot U(s) = \frac{FS}{s(\tau s + 1)} = \frac{FS}{\tau} \frac{1}{s \left( s + \frac{1}{\tau} \right)} \quad (3)$$

By doing the inverse Laplace transformation:

$$y(t) = FS (1 - e^{-\frac{t}{\tau}}) \quad (4)$$

Evaluating  $y(t)$  at  $t = 1$  s:

$$y(t = 1[s]) = FS \left( 1 - e^{-\frac{1[s]}{\tau}} \right) = 0.9 \cdot FS \quad (5)$$

$$(5) \rightarrow 0,1 = e^{-\frac{1[s]}{\tau}} \rightarrow \tau = -\frac{1}{\ln(0,1)} [s] \quad (6)$$

By multiplying the physical signal with sensor's (first order system) dynamics, an estimate for the sensor's analog output signal can be obtained. Sensor dynamics is used when flow rate calculated from piston velocity and pressure values is compared with flow rate from flow sensors.

### 3.1.5 Actuators

Test o consisted of several tests. Tests differ from each other on the actuator that was used. In *Table 1* the actuators' specifications are reported, and actuators are named.

Three set of tests were done:

- Test 0.1: two actuators 1 positioned in parallel
- Test 0.2: one actuator 1
- Test 0.3: one actuator 2

### **3.1.6 Other components**

The team had to understand how to test the system with the same amount of CA. To ensure enough CA, two 30 liters tanks were installed.

To avoid back flow a check valve was installed at the inlet of the tanks.

In tests it was chosen that the actuators should have similar velocities in both experiments (with and without the unit). The backpressure generated by PESU is higher than the pressure loss generated by the silencer of traditional systems.

This resulted in actuators having a greater speed when the unit was not applied. To ensure that the actuators had similar speed, the out-flow of the cylinder had to be throttled when the unit was not applied to the CAS. Two throttling valves were applied to the system, one for each actuator inlet.

Once an experiment was terminated, i.e., the pressure present in the system is too low to move the actuators, some residual pressure is still present in the system. If the system had to be tested with and without the unit, the unit had to be unplugged from the system. This meant that tubes were to be unjointed from their fittings. Since the unit was generating some backpressure, residual pressure values were different according to if the system was tested with or without the unit. If the system had to be tested with the same amount of air, by imposing atmospheric pressure in the tube was the only way to ensure the same value of residual pressure for each test.

To do so tubes had to be unplugged and CA to be exhausted in the environment. Once ambient pressure was reached in the tubes, they could be plugged back in. Apart it being a very tedious procedure, exhausting CA can choke the tube ending. The tube will act like a nozzle. When choked, a nozzle generates soundwaves which are unpleasant and painful for the human ear.

By inserting exhaust valves with muffler in each section of the system, the team was able to exhaust leftover CA in safety. In total five exhaust valves were present in the system.

In Table 1 a more detailed description of the components used is given.

Table 1: Components' specifications.

<b>nomenclature</b>	<b>Component</b>	<b>Code/manufacturer</b>	<b>Specs</b>
<b>1A</b>	Shut-off valve with exhaust port	EVHS3500-F02-X116	
<b>1B</b>		VHS40-F04B	
<b>1c</b>		VHS40-F04A	
<b>2A</b>	Air filters	AW40-F04E-B	Oil filter
<b>2B</b>		AFD40-F04-A	Vapor filter
<b>2C</b>		AW40K-F04-B	Oil filter
<b>2D</b>		AFM40-F04D-A	Oil filter
<b>2E</b>		AFM40-F04-A	Oil filter
<b>3</b>	Check valve	AK2000	
<b>4</b>	Air tank	PREMI	Volume 30[l]
<b>5</b>	Stop valve	PN500	
<b>6A</b>	Reed sensor	D-A93	
<b>6B</b>	Position sensor	0007446 SGH10	
<b>7</b>	5/3 directional control valve	SY9320-5YZ-03F-Q	
<b>8</b>	Speed control valve	AS3002F	
<b>9</b>	Silencer	AN200	
<b>P</b>	Pressure sensor	PSE530-M5	
<b>T</b>	Temperature sensor	20073657	
<b>Q<sub>1</sub></b>	Flow meter	PF2MC7501-F04-D-M	5-500[l/min]
<b>Q<sub>2</sub></b>		PFMC7102-F04-E	10-1000[l/min]
<b>Q<sub>3</sub></b>		PFMC7501-F04-E	5-500[l/min]
<b>Actuator 1</b>	Double acting cylinder	CP96SDB80-700C	Stroke 700[mm] Bore 80[mm]
<b>Actuator 2</b>	Double acting cylinder	ECDQ2A40-25DM	Stroke 25[mm] Bore 40[mm]
<b>Actuator 3</b>	Dual rod, Double acting cylinder	CXSL32-100	Stroke 100[mm] Bore 32[mm]
<b>Actuator 4</b>	Double acting cylinder	MKA32-20LN	Stroke 20[mm] Bore 32[mm]
<b>G</b>	Gripper	MHM-25D	
<b>90</b>	Elbow union		
<b>3w</b>	Union tee		

### 3.2 Test 1's system

Once the course was concluded, further tests were set to be implemented.

First the system was modified as seen in *Figure 6*. Tubes were shortened to avoid dissipation. Shut off valve (number 5) was removed and substituted with an exhaust valve (third valve starting from the system supply). Pres-



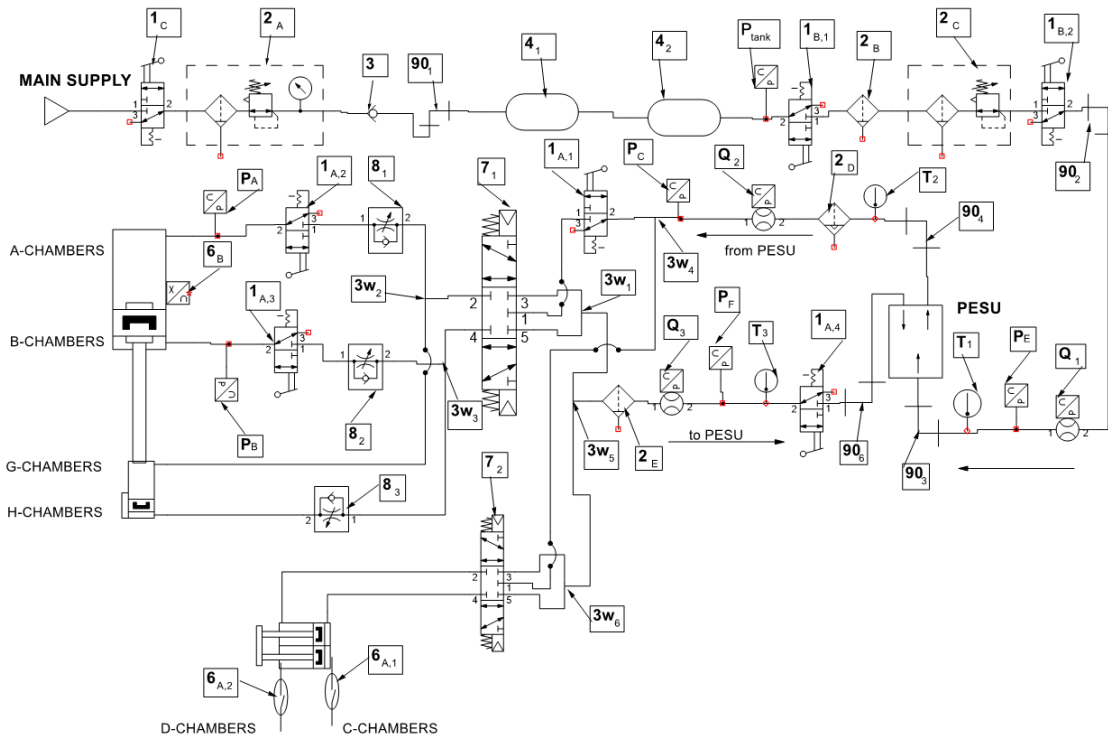


Figure 8: packaging system with PESU.

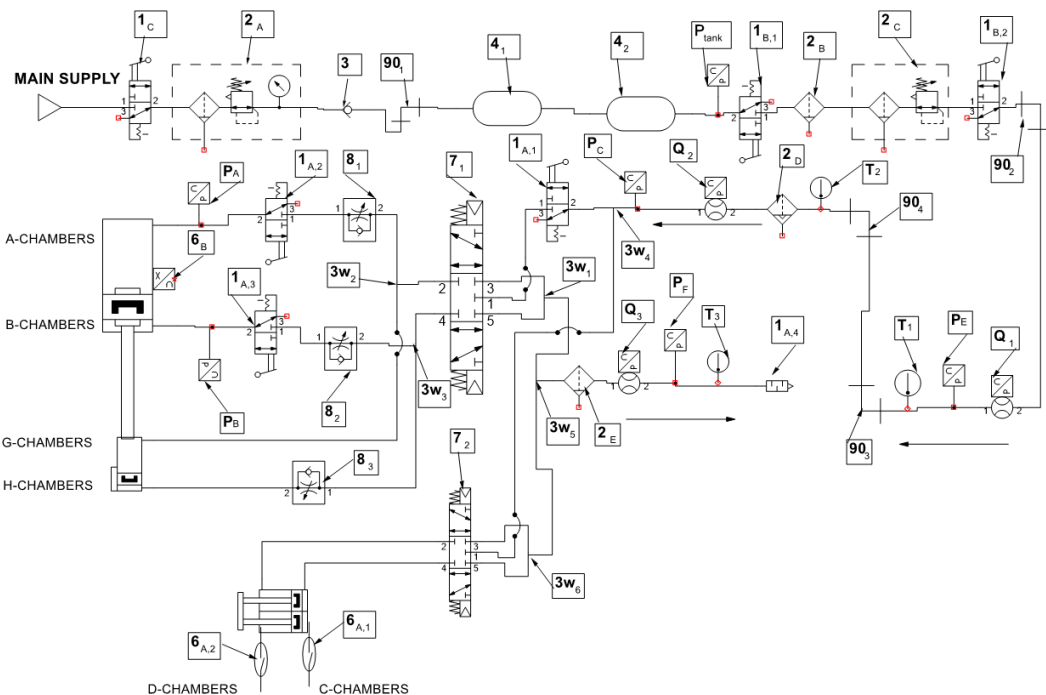


Figure 9: packaging system without PESU.

The system is designed to pick up a small metallic object from the ground and store it in a little box (magnetic grippers can only gasp on metallic objects). The box is located at the end of actuator 3 end. The design of the sys-

tem was done with components present in the lab. For the metallic object to be stored under actuator 1, the box had to be positioned under actuator 1. When actuator 1 elongated, the box must not have been present under actuator 1. Thus, the actuator stroke had to be longer than the box length. Being the smallest box in the lab 90 mm in length, double piston actuator CXSL32-100 (100 mm stroke) was chosen.

### **3.3.1 Magnetic gripper**

The system was designed to activate the gripper when actuator 1 is in position B, and to deactivate when actuator 1 is in position A. The area ratio in the gripper is different than in actuator 1. As recorded data in *Figure 29* shows,  $P_B > P_A$  in most of the cases. If pressure would be taken directly from the supply for actuator 1 chambers, the gripper would always be inactive. A throttle valve is restricting flow going to the deactivation side of the gripper. This way  $P_G$  (pressure values present in the gripper's chamber connected to actuator's B chamber) would be lower than  $P_B$  when actuator 1 was retracting. Thus, the gripper was in the active position when actuator 1 was retracting.

### **3.4 Test 3's system**

This test was meant to analyze the effect of the unit at low flow rate values. An actuator with smaller rod diameter was then needed. Choosing from what was available in the lab, actuator 4 was chosen.

The system is almost the same as the one in test 1, just actuator 1 was substituted with actuator 4.

### **3.5 External power supply**

At first the team was intentioned to use a compressor present in the lab. Unfortunately, this compressor proven to be too noisy. It was then chosen to use the lab's CAS, which offered safer applications. Measuring power consumption of such a source is complex because the compressor was used by other research teams, also. It was preferred to measure total energy consumption though a method described in chapter 7.1 .

## 4 Tests system description

Following the design described in above section, the tests' system was built. The system can be seen in *Figure 10*.

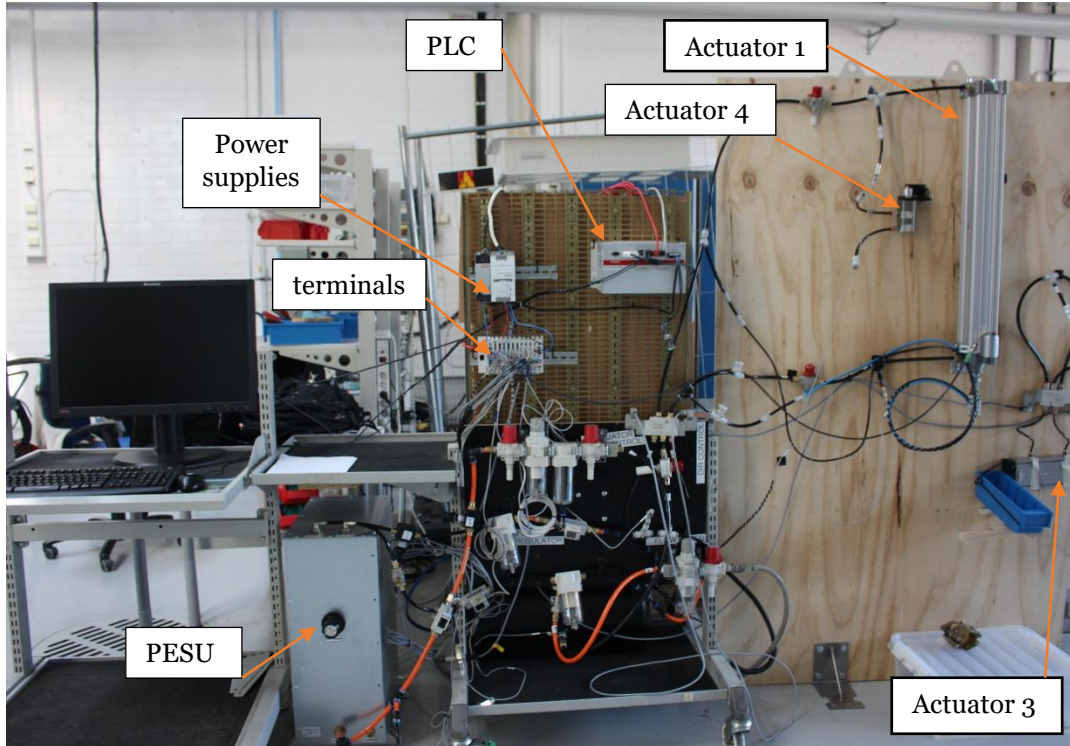


*Figure 10: picture of the system.*

One system was built for all the type of tests and experiments. When the unit had to be disconnected from the system, connection leading to it were disconnected. The tube where flow was directed from the supply to the unit, was connected via a diameter adapter (the two tubes had different diameters) to the tube where flow was directed from the unit to the valves. Flow was exhausted by flipping the shut of valve positioned on tube going from valves to the unit.

When actuator 3 had to be connected, a 90-degree fitting was substituted with a three-port fitting. To connect actuator 4, tubes connected to actuator 1 were disconnected and connected to actuator 4 instead.

### 4.1 Terminal wiring

All sensors were powered via Beckhoff's terminals by using external power source. analogical signals were read by using Beckhoff's input terminals and

forwarded to the PLC via an EtherCAT cable. In the PLC signals values were then translated to give them their real physical values.

An almost continuous reading was given by the PLC, which read data with sampling frequency of 100 Hz. The sampling frequency was enough to fulfil the Nyquist frequency since no high frequency phenomena were present in the measured signals. In the PLC the inbuilt a programmable low pass filter was set to 50 kHz. Neither the less noise in the signal was present.

## **4.2 Pneumatic system**

When building the system, attention was paid to minimizing dissipation and space usage. Tubes were selected with the highest diameters available in the laboratory. Flexible polyurethane tubes were used: 12x8 mm (TU1208), 6x4 mm (TU0604) and 10x6.5 mm tubes (TU1065). 90-degree fittings were avoided where possible. The tubes and their dimensions are presented in Table 2.

To modify the system from test 2 to test 1 or 3, three-way valves  $3w_4$  and  $3w_5$  were substituted with 90-degree fittings  $90_5$  and  $90_7$ . To disconnect the gripper, the three-way valves  $3w_2$  and  $3w_3$  were substituted by linear connectors.

Components had to be kept stationary and avoid oscillations. When possible, components, as filter and exhaust valves were either screwed onto the wood support behind or tied with cable ties. To have a clear and well-organized workspace, sensors' wires were kept as short as possible.

Table 2: lengths of connections between components.<sup>1,2</sup>

components	Length [cm]	Tube diameter [mm]	components	Length [cm]	Tube diameter [mm]
<b>2A-3</b>	60	12	<b>P<sub>B</sub>-1A<sub>3</sub></b>	15	10
<b>3-4<sub>1</sub></b>	50	12	<b>1A<sub>3</sub>-8<sub>2</sub></b>	20	10
<b>4<sub>1</sub>-4<sub>2</sub></b>	90	12	<b>8<sub>2</sub>-3W<sub>3</sub></b>	5	10
<b>P<sub>T</sub>-1B<sub>1</sub></b>	100	12	<b>3W<sub>3</sub>-7<sub>1</sub></b>	18	10
<b>1B<sub>2</sub>-90<sub>1</sub></b>	20	12	<b>7<sub>1</sub>-3W<sub>1</sub></b>	40	10
<b>90<sub>1</sub>-Q<sub>1</sub></b>	5	12	<b>3W<sub>1</sub>-3W<sub>5</sub></b>	16	10
<b>Q<sub>1</sub>-P<sub>E</sub></b>	20	12	<b>3W<sub>5</sub>-2E</b>	20	10
<b>P<sub>E</sub>-T<sub>1</sub></b>	20	12	<b>2E-Q<sub>3</sub></b>	20	10
<b>T<sub>1</sub>-90<sub>3</sub></b>	20	12	<b>Q<sub>3</sub>-P<sub>F</sub></b>	5	10
<b>90<sub>4</sub>-T<sub>2</sub></b>	25	10	<b>P<sub>F</sub>-T<sub>3</sub></b>	5	10
<b>T<sub>2</sub>-2D</b>	20	10	<b>T<sub>3</sub>-1A<sub>4</sub></b>	10	10
<b>2D-Q<sub>2</sub></b>	12	12	<b>1A<sub>4</sub>-90<sub>6</sub></b>	20	10
<b>Q<sub>2</sub>-P<sub>C</sub></b>	10	10	<b>3W<sub>4</sub>-7<sub>2</sub></b>	190	10
<b>P<sub>C</sub>-3W<sub>4</sub></b>	5	10	<b>7<sub>2</sub>-Act<sub>3</sub></b>	15	6
<b>3W<sub>1</sub>-1A<sub>1</sub></b>	13	10	<b>Act<sub>3</sub>-7<sub>2</sub></b>	180	6
<b>1A<sub>1</sub>-7<sub>1</sub></b>	5	10	<b>7<sub>2</sub>-3W<sub>6</sub></b>	40	10
<b>7<sub>1</sub>-3W<sub>2</sub></b>	50	10	<b>3W<sub>6</sub>-3W<sub>5</sub></b>	190	10
<b>3W<sub>3</sub>-8<sub>1</sub></b>	20	10	<b>3W<sub>2</sub>-G</b>	190	10
<b>8<sub>1</sub>-1A<sub>2</sub></b>	20	10	<b>G-3W<sub>3</sub></b>	190	10
<b>1A<sub>2</sub>-P<sub>A</sub></b>	25	10	<b>P<sub>A</sub>-Act<sub>4</sub></b>	10	6
<b>P<sub>A</sub>-Act<sub>1</sub></b>	10	10	<b>Act<sub>4</sub>-P<sub>B</sub></b>	20	6
<b>Act<sub>1</sub>-P<sub>B</sub></b>	25	10			

<sup>1</sup> Reported connection's length between components are including of fitting length's

<sup>2</sup> If not reported, distance between two components is equal to zero.

## 5 Control algorithm

As for the pneumatic, also the control algorithm was first developed during mechatronics course. Then it was modified and improved after the course.

The control algorithm was developed on Beckhoff coding environment. Developing the control algorithm can be divided in two phases: obtaining sensors' data to the PLC and developing the control code.

Tests had to be done using an industrial C.A. pressure range. It was chosen to test the systems only when the pressure at the tank was between 4 to 6,5 bars which is a pressure range compatible to the one normally used in industry. Before initiating the movement, pressure at the tank had to be higher than 6.5 bars. Once this statement was true, the movement algorithm could be initiated. If tank pressure fell under 4 bars, the movement algorithm was terminated. Actuators would stop because no CA was supplied to them. The movement algorithm could be initialized again if the pressure at the tank would rise over 6 bars. When the movement algorithm was not active, no power was given to the directional control valves. If no power was given, directional control valves were in the middle position, i.e., the lock position, thus not allowing the flow of air to the actuators.

A safety switch was also implemented. If the pressure in the system would rise higher than what the components can withstand, the directional control valve would move to the lock position.

The pressure range control and the safety switch were common to all control algorithm in the tests.

## 5.1 Test 0's control algorithm

The control algorithm for test 0 is present in *Figure 11*.

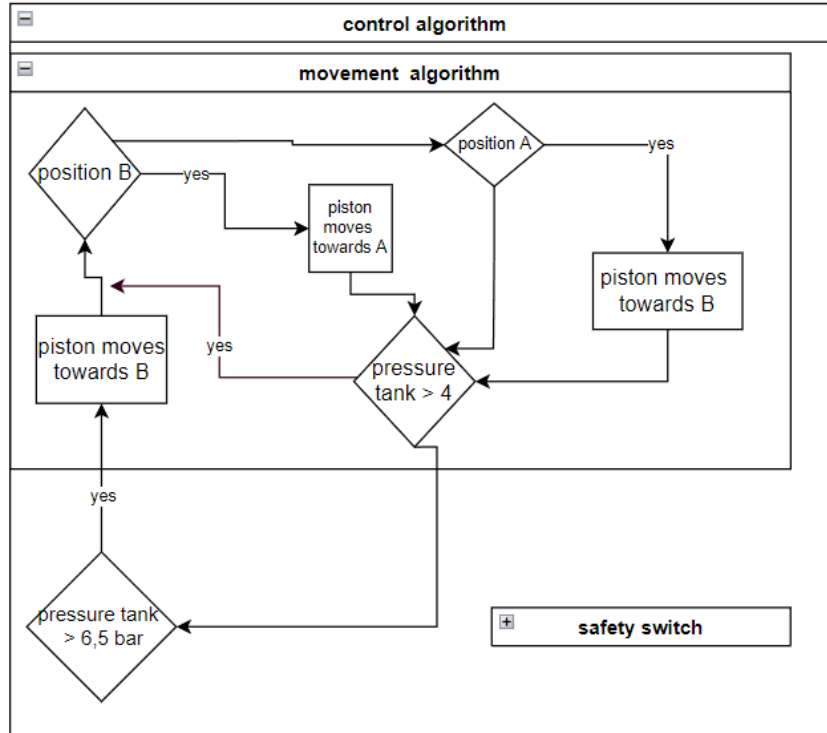


*Figure 11: Control algorithm scheme.*

At the beginning of the experiment, the actuator was always positioned in its cap end position. When the movement algorithm was initiated, the actuator was always moved towards head end.

According to the reed sensor's signal, the piston's position was detected. When the PLC detected signal from one of the reed sensors, the control algorithm would actuate the directional control valve to make the piston reach the opposite position.

## 5.2 Test 1's control algorithm

Regarding the control algorithm, no major changes were applied with the respect to test 0. The only difference consisted of how way the piston position was detected.

### 5.2.1 Position sensors

Previously the piston end positions were detected via reed sensors. In the upgraded version of the system a position sensor is used. The position sensor, a draw-wire encoder (which was previously not available) was attached to the rod's end and it read the relative piston position. The zero position was set to one end of the rod, while the full length of the stroke was set to the other end of the piston. When the sensor read a value corresponding to zero or to the stroke length, then it could be assumed that the piston was in one of the two end positions. Thus, the position sensor was working like a reed sensor (reed switch). The wire sensor's setup is presented in *Figure 12*.



*Figure 12: position sensor setup.*

The complete elongation of the piston was only reachable few seconds after the rod had reached the value of 690 mm (the total stroke length is 700 mm). In fact, to avoid collision between the piston and the cylinder internal

ends, close to the end position the cylinder activates end of stroke cushioning.

To account for that, the zero position was considered when the position sensor reached a value of 4 mm while the top position was set to the value of 690 mm.

A major advantage of setting the end of stroke before the actual zero position was reached was the gain in system dynamics. The algorithm was designed as such that when a certain condition was reached (a specific value was reached in the case of the position sensor or an analog signal in the case of reed sensors) the directional control valve was actuated in the opposite direction. Actuating the valve and waiting for the CA to reverse its flowing direction generated a small delay (which was not evaluated). If the zero position was set before the actual zero position was reached, then, for a small amount of time, the rod would still be actuated in its previous direction. This can be seen in the recorded data, where the position sensor reaches values in the decimal close to zero. The end stroke values were obtained by experimental analysis.

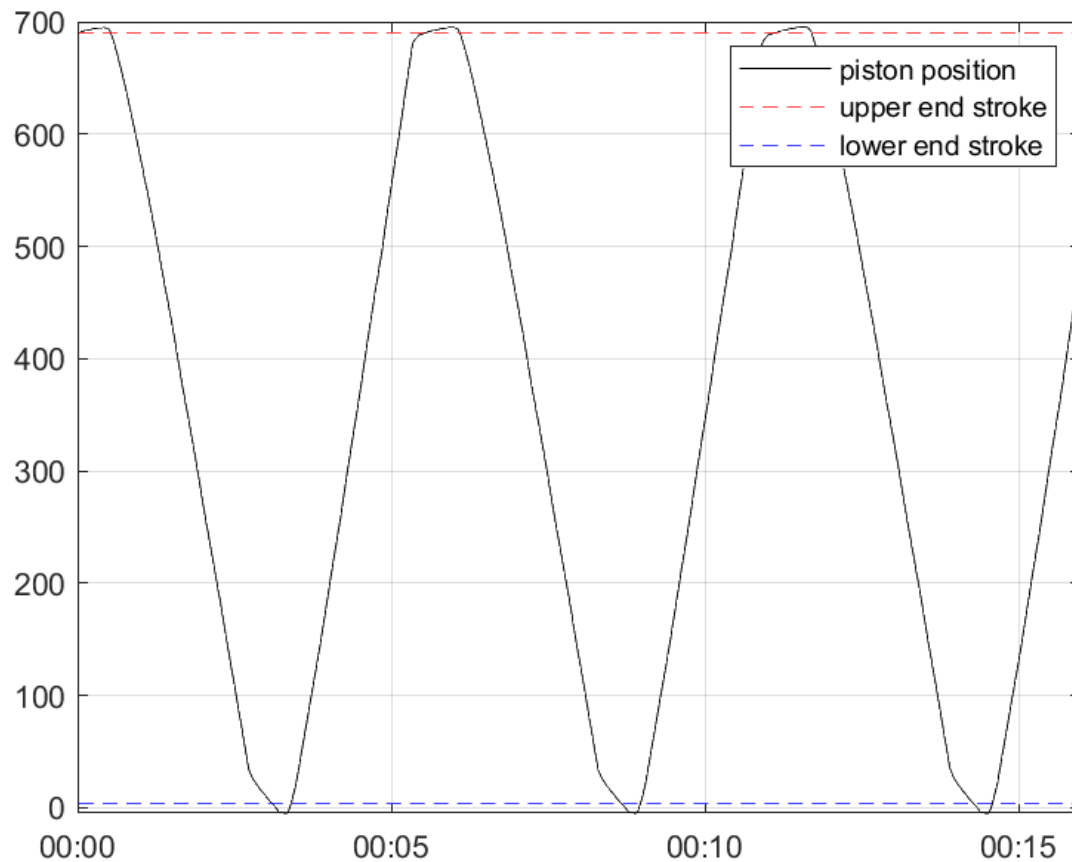


Figure 13: position plot.

In *Figure 13* position readings are shown. After either the upper or lower end stroke position has been reached, the piston is still moving. In the upper position it does not reach the end stroke position (700 mm) reading. On the other hand, the end stroke position is reached in the lower position (the 0 mm reading). The position reading in the low position gives a minimum of -4 mm reading, which is caused by an error when setting the zero point, while the upper position gives a maximum reading of 696 mm.

In general, there seems to be a greater delay when moving towards the lower position than the opposite. Moving towards the upper position requires higher flow rate value than moving towards the lower position. Chamber A has a greater volume than chamber B. An explanation to this delay could be that, to achieve greater flow rate, more time must pass for the fluid to properly pressurize the volume in chamber A, and to compensate the pressure in chamber B.

Also, the piston seems to slow down faster when moving towards the lower position. This speed decrease is also present in the other direction, but it begins closer to the upper end stroke. This is caused by the pressure cushion, which, hinders flow rates while in the latest stages of exhaustion.

It must be mentioned that the zero and full-length position could also be achieved when the piston had not reached its respective end. As said, the position sensor's wire was attached, via a small screw, to the piston end via a small support. The piston had a circular base area, and, when piston was actuated, the rod could rotate on its central axis, generating an unwanted and dangerous behavior. If the rod was rotating, the support of the position sensor's wire, which sticks out of 9 mm from the piston's center, would rotate as well. When rotating it could collide with other parts of the system. Secondly, if the wire support would rotate but the position sensor would not move, the wire would no more be in a straight line. The wire would be bending. There wouldn't be any more linear relation between the drawn wire length and the piston's position. This would mean that the drawn wire's length would be more with the respect to expected amount of drawn wire of the same position. Readings would not be reliable.

In every experiment the tester made sure that the rod wouldn't turn.

### 5.3 Test 2's control algorithm

Controlling this system required a more complex algorithm. Actuator 1 and actuator 3 are controlled to avoid collision between each other. The control algorithm is presented in Figure 14.

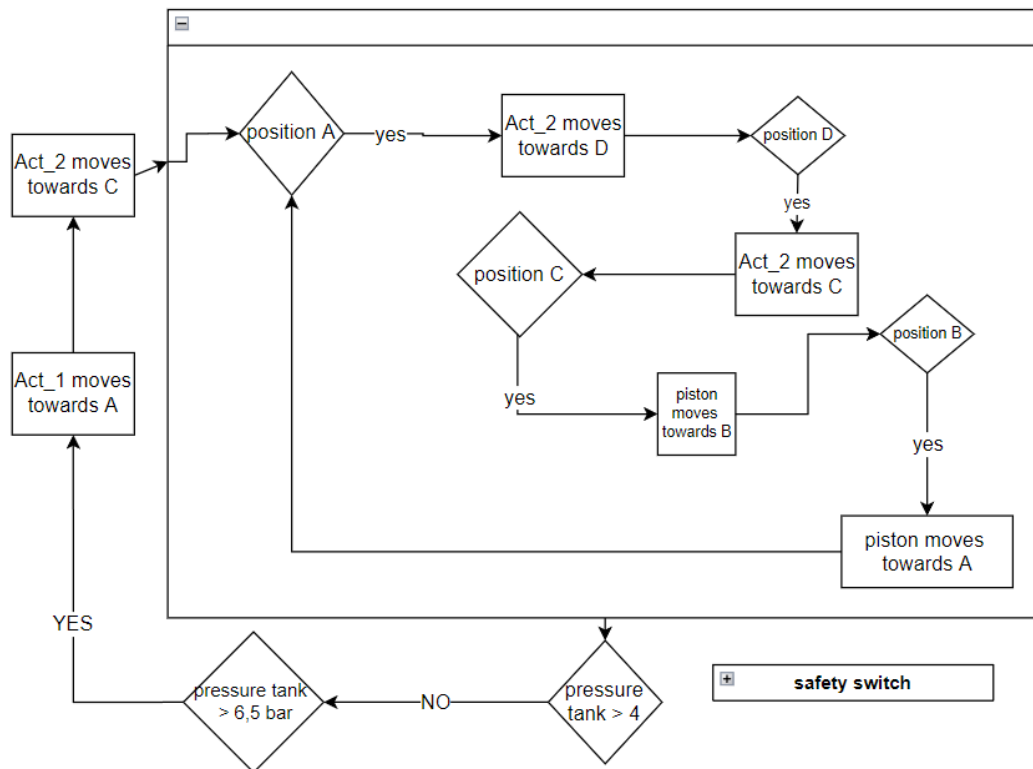


Figure 14: control scheme test 2.

When the pressure sensor at the tank reads a value higher than 6.5 bars, the movement of the system is initiated. Before initiating the movement algorithm, Actuator 1 is moved to the position A while actuator 3 is moved to position C. As such the starting position of every actuator is always known and collision between the two actuators is avoided.

Once actuator 1 reaches position A, the gripping action takes place. In theory every actuator would need a controllable driver. That would have required an additional output terminal, which was not available. The gripper activation\deactivation is controlled as described in chapter 3.3.1.

The control system does not check if the gripper has been activated. Once position A has reached, a signal is given to the directional control valve moving actuator 1 towards position B. No delay is inserted by software. The delay present in the system is enough for the gripper to grasp the product needed to move.

### **5.3.1 Test 2 movement description**

The system phases are shown in Figure 15, Figure 16, Figure 17 and Figure 18. First, in phase 0, actuator 1 is moved from position A to position B. In phase one actuator 1 reached position B (Figure 15), i.e., the extended position. The gripper was activated, and the metallic object was attached to the gripper.

In phase two actuator 1 reaches position A (Figure 15) i.e., the full retract position. Thanks to the delay generated by the throttle valve, the gripper is still active.

In phase 3 actuator 3 moves to position D (Figure 17) under actuator 1 to collect the metallic object. The gripper deactivates and the metallic object falls in the box.

Finally in phase 4 Actuator 3 retracts towards position C. Once position C is reached, the cycle is considered concluded. Actuators are in conditions of phase 0. The cycle can be initialized again.

### **5.4 Test 3's control algorithm**

Dealing with one piston only, no changes were made to the control algorithm. The only difference is that end stroke positions were detected via two reed sensors instead than setting the end strokes to specific reading from one position sensor. The control algorithm is identical to the one of Test 0.

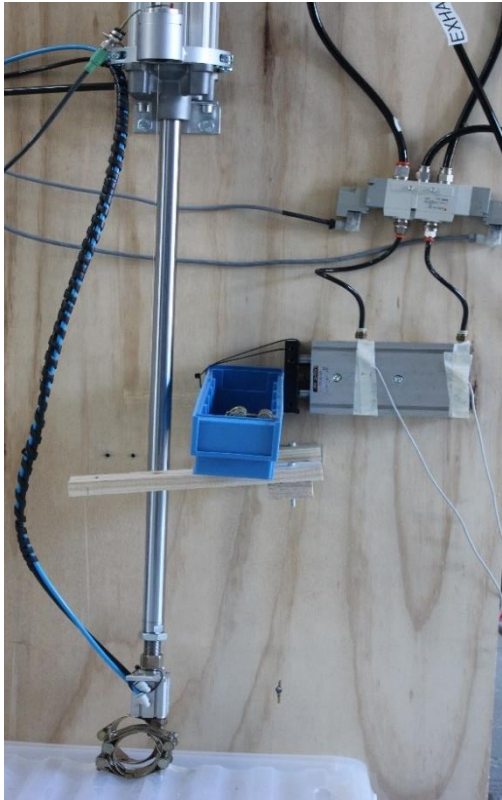


Figure 15: Phase one.



Figure 16: Phase two.



Figure 17: Phase three.



Figure 18: Phase four.

## 6 Tests

All gathered data were collected through the PLC.

Once the experiments conditions were set up, i.e., the system was connected according to the intended experiment, the system was pressurized. Beckhoff's PLC allows to record data for a maximum of 10 minutes. This gave the possibility to record data before and after the experiments took place.

In Beckhoff's PLC recording data is done by selecting variables to display on TWINcat 3 scope extension. The user sets recorded variables. When a variable is recorded, the software displays it on the scope interface.

While the software is running, reading values, and giving commands to outputs terminals, the software can display data with no noticeable delay.

Once the experiment is terminated or high enough data values have been gathered, the acquisition can be terminated without having the control algorithm to log out from the PLC. This way the PLC is still controlling the system without interfering with the data recordings.

Once data have been acquired, they are saved in a svdx file (scope data file). Now data are saved and ready to be analyzed. In this thesis it was chosen to post process data through MATLAB which is not able to read .svdx files. The data must first be exported in .csv (comma separated value) file. This can be done by the dedicated export window on TWINcat.

When exporting from .svdx to .csv and when processing data on MATLAB, a time range can be chosen. Test 0 had a specific test procedure, while tests 1,2, and 3 followed the same procedure.

### 6.1 Test 0 test procedure

In test 0, the team tested the effect of PESU in the system with the same amount of CA. The same system was tested with and without PESU. To do so the system was first filled up with CA at 7 bars, then the system was tested.

To ensure that the same amount of CA was stored in the systems, it was chosen to undertake the following procedure:

1. Stop valve (5) was closed, the tank side of the system was then isolated from the rest of the system.
2. Shut-off valve (1) was opened.
3. When tank pressure sensor was reading 7 bars, shut-off valve (1) was closed.

Now the system contained the desired amount of CA. Recording of parameters was initiated and stop valve (5) was opened.

## 6.2 Test 1, 2 & 3 recording procedure

The amount of time taken by the systems to complete one cycle in all tests was always less than 10 seconds. It was then decided to record data for 3 minutes. This would have meant that the system would have done enough cycles to evaluate overall performance.

But data were not analyzed on the whole sampled time span. To have reliable readings, quantities as pressure and temperature had to reach stable values. It was then chosen to start analyzing data after 50 seconds of the recording's beginning. Data were sampled up to the first time the actuator reached one of its end stroke positions and 2:50 minutes passed from the beginning of the recording. So, the sampled time span went from 50 seconds to 170 seconds plus the time taken for the actuator to reach its final position.

Recording was initiated right after the system finished its first cycle.

Cycles took always less than 10 seconds. Showing measurements for the whole-time span would have meant to analyzed so much data that it would have been hard to interpret. Variables are then showed on a selected time range which varies upon the graph. All graphs report data starting 50 seconds the recording's beginning.

## 6.3 Checking mass flow rates

The validity of recorded data was done by matching mass flow rates. Mass flow rates values calculated from the flow metering sensors were matched with flow rate value calculated from piston velocity. This way it can be check if recorded piston velocity's values and pressure value at the actuator are consistent with measured volumetric flow reading from flow sensors.

As it will be explained in subparagraph 8.5, when PESU is utilized, pressure  $P_c$  experiences some sudden increase, thus not providing quasi-steady state values. To best verify the validity of measured data, it was chosen to use data gathered without PESU. This is valid also for subparagraph 6.4, where data have been validated using the measurements without the use of PESU.

It is known that mass flow rates of any fluid can be calculated by:

$$\dot{m} = \dot{x} \cdot A \cdot \rho \quad (7)$$

In CA air is used working fluid. Air is a compressible fluid, meaning that density is not constant, but is dependent on temperature and pressure. If air is considered an ideal gas, then:

$$\rho = \frac{P}{R \cdot T} \quad (8)$$

Then, mass flow rate can be written as:

$$\dot{m} = Q \cdot \frac{P}{R \cdot T} = \dot{x} \cdot A \cdot \frac{P}{R \cdot T} \quad (9)$$

Air gas constant  $R=287$  [J/(kg\*K)]. With this data the mass flow rate can be calculated. In the case of  $\dot{m}_2$  being the mass flow rate supplied to the actuator and  $\dot{m}_3$  being the mass flow rate exhausted by the actuator:

$$\dot{m}_2 = Q_2 \cdot \frac{P_0}{R \cdot T_0} \quad (10) \quad \dot{m}_3 = Q_3 \cdot \frac{P_0}{R \cdot T_0} \quad (11)$$

The mass flow rates can be matched with the mass flow rate values calculated by using the piston velocity.

Only test 1 is suitable for this match. Both Test 2 and test 3 have actuators controlled via position switches. Position switches are not suitable since they won't give reliable information about piston's velocity. A rough estimation of the velocity can be given by dividing the stroke by the time taken. Unluckily piston's velocity is not constant over the stroke. This would lead to some information's losses in actuator 3 and 4 velocity values. In test 1 position is controlled by the position sensor.

Velocity is obtained by numerically deriving the position sensor readings. It was done using an open-source first-order finite-difference method MATLAB code (19). No velocity sensor was available.

From theory it is known that if the piston velocity is multiplied by the piston's area, the flow rate can be calculated.

The mass flow rate can be estimated by multiplying the piston velocity by the corresponding piston area. This (quasi-steady) calculation does not include the flow rate components related to the changes in cylinder pressures. When the piston is moving toward position B, the inlet flow can be calculated by multiplying the absolute velocity value by  $A_A$ . The outflow can be instead calculated by multiplying the absolute velocity value with  $A_B$ . When the piston is moving toward position A, the input flow is calculated via  $A_B$  and the output flow is calculated via  $A_A$ .

To calculate the mass flow rates, flow rates are multiplied by the relative pressure and temperature values. Pressure values ( $P_A$  relative to  $A_A$  and  $P_B$  relative to  $A_B$ .) are not available in the chambers. Pressure values are sampled immediately outside the actuators using a 3-way port pneumatic fitting. Sensor reports pressure values in gauge pressure. To calculate mass

flow rates,  $P_0$  must be added to sensors' pressure values. Temperature values at the actuators are not sampled. It is assumed as  $T^* = 25^\circ\text{C}$ . Temperature does not change dramatically over time (chapter 8.7). Temperature values are always assumed to be equal to temperature values at standard conditions.

Thus, if  $\dot{x} > 0$ :

$$\dot{m}_{3,cal} = Q_3 \cdot \rho = \dot{x} \cdot A_A \cdot \frac{(P_A + P_0)}{RT^*} \quad (12)$$

$$\dot{m}_{2,cal} = Q_2 \cdot \rho = \dot{x} \cdot A_B \cdot \frac{(P_B + P_0)}{RT^*} \quad (13)$$

If  $\dot{x} < 0$ :

$$\dot{m}_{3,cal} = Q_3 \cdot \rho = -\dot{x} \cdot A_B \cdot \frac{(P_B + P_0)}{RT^*} \quad (14)$$

$$\dot{m}_{2,cal} = Q_2 \cdot \rho = -\dot{x} \cdot A_A \cdot \frac{(P_A + P_0)}{RT^*} \quad (15)$$

The flow sensors have an error of  $\pm 3\%$  over FS. In the case of  $\dot{m}_2$  the maximum reading is 1000 [L/min], while for  $\dot{m}_3$  is 500 [L/min]. The mass flow rates calculated via piston's velocity should be in the range of the error of the flow rates sensors. The maximum allowed error depends on the flow meter. Is calculated as:

$$e_{max,m_2} = 1000 \cdot 10^{-3} \cdot \frac{P_0}{R \cdot T^*} \quad (16) \quad e_{max,m_3} = 500 \cdot 10^{-3} \cdot \frac{P_0}{R \cdot T^*} \quad (17)$$

Given that the error on  $\dot{m}_2$  is double with the respect to the one of  $\dot{m}_3$ , it was chosen to show results only for  $\dot{m}_3$ . This way results could be analyzed in the safest conditions. Results regarding  $\dot{m}_2$  are reported in the appendix in Figure 42 and Figure 43.

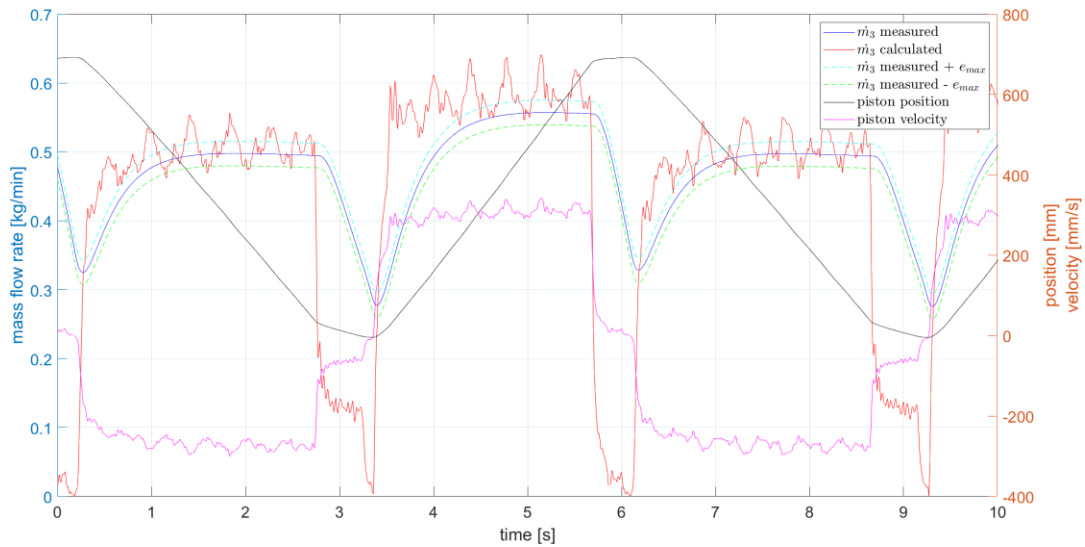


**Figure 19: comparing mass flow rate 3 from sensor readings to the calculated from piston's velocity when the unit is applied.**

In Figure 19 the two mass flow rates are compared. The calculated flow rate is almost never in the range of the error. The two curves show similar magnitude. This is because the two mass flow rates are not comparable. There is a delay between the flow rates measured by the sensors and the calculated one.

To properly compare the two mass flow rates the flow metering valve's delay had to be taken in consideration. Calculated mass flow rates are first divided by  $\rho_0$  (from equation (8)  $\rho_0 = P_0 / (R \cdot T_0)$ ) to obtain volumetric flow rate at standard condition (the output of flow sensor). The calculated volumetric flow rate is then multiplied by the flow sensor's delay. The obtained signal is then multiplied by  $\rho_0$ . These mass flow rates are then used to evaluate the total amount of air.

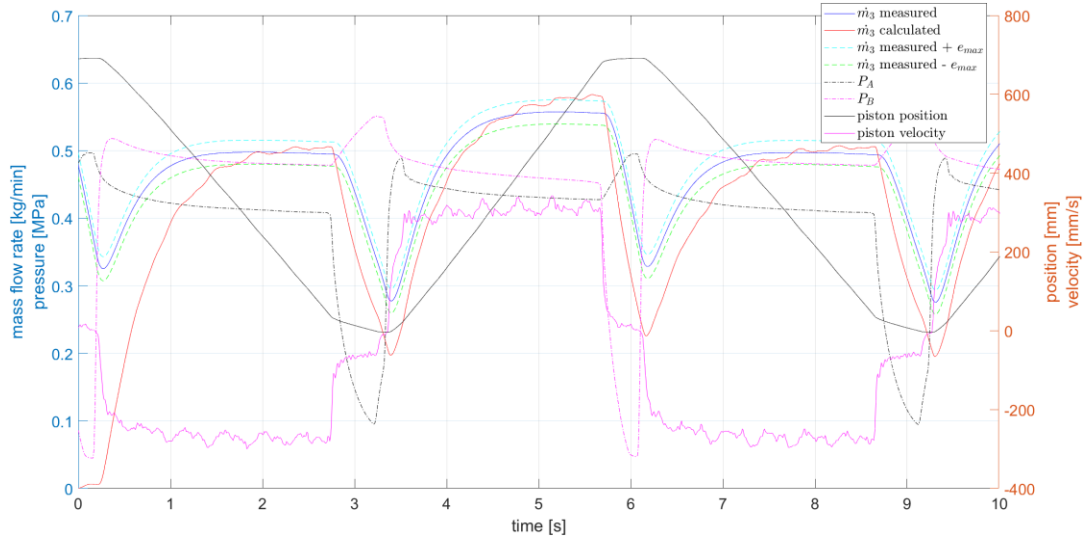


Figure 20: values reported in Figure 19 with sensor dynamics.

In Figure 20 calculated and measured mass flow rate are compared taking in consideration sensor's delay. The two mass flow rates are consistent with each other (red line is included in between the sensor's error) only when velocity and pressure values in the actuators are in quasi-steady state. In the cycle's beginning and end the calculated flow rate is not found in between the error range. This is most likely due to effect of air compression which were ignored.

Figure 20 demonstrates that flow rates are consistent only in some time instants. This is expected since pressure transient are difficult to represent with the used system design.

To farther evaluated if the overall measured flow rate is consistent it was chosen to compare the total amount of used CA and see if it falls in the range of the error.

Mass flow rates were integrated over time. Integration of mass flow rates was done in MATLAB via the inbuilt trapezoidal method function. When comparing the difference between the readings of two sensor, the maximum allowed error is taken as the major of the two.

Table 3: error in total mass calculations.

	$ m_2 - m_3  = [\text{kg}]$	$ m_2 - m_{2,cal}  = [\text{kg}]$	$ m_3 - m_{3,cal}  = [\text{kg}]$
<b>With PESU</b>	0.015	0.087	0.037
<b>Without PESU</b>	0.010	0.123	0.065
$e_{max} = [\text{kg}]$	0.073	0.145	0.072

As it can be seen from Table 3, all the error values are lower than the maximum error. Mass flow rate values are considered consistent.

## 6.4 Checking pressure drops

In chapter 6.3 the validity of volumetric flow rates values was checked. In this chapter the validity of pressure drops is checked.

From theory it is known that mass flow rates values through an orifice can be calculated. It can only be done if fluid state variables and geometrical parameters are known (pressure values at the orifice's inlet and at the outlet, temperature at the inlet, geometry parameters and critical pressure ratio).

SMC at page 29 of (20) using ISO 6358: 1989 (21) gives a simple method to evaluate the flow rate at standard condition through a pneumatic component.

Given:

$$P_{ratio} = \frac{P_2 + P_0}{P_1 + P_0} \quad (18) \quad B = \frac{P_{cr} + P_0}{P_1 + P_0} \quad (19)$$

Sonic conductance C and fluid temperature T, it is known that:

If  $B < P_{ratio}$

$$Q = 600 \cdot C \cdot (P_1 + 0,1) \sqrt{\frac{293}{273 + T}} = [\text{L/min}] \quad (20)$$

If  $B \geq P_{ratio}$

$$Q = 600 \cdot C \cdot (P_1 + 0,1) \sqrt{1 - \left(\frac{P_{ratio} - B}{1 - B}\right)^2} \sqrt{\frac{293}{273 + T}} = [\text{L/min}] \quad (21)$$

To evaluate if pressure drops were consistent with flow rates values, just results from test 1 were analyzed.

In test 1 six pressure sensors were present. Flow rates' parameters (B and C) could only be evaluated where the mass flow rate in between two pressure drops was not affected by leakages or moving parts.

PESU is recirculating air through a pneumatic booster, a component with moving pistons producing alternating volumetric flow rate. Volumetric flow rate to valve ( $Q_1$ ) is not linearly dependent on the value of inlet pressure. Pressure drops in between PESU cannot be used to evaluate the flow rates in between the unit. No direct flow crosses the actuator. Flow parameters between  $P_T$  and  $P_E$  could not be evaluated. Component 2c contains a pressure regulator. According to the inlet pressure values and to the set maximum pressure values, a pressure regulator modifies its geometry to reduce

the pressure of the flow leaving the unit. Thus, a pressure regulator changes geometry and flow parameter according to the fluid status. To evaluate flow parameters geometry should remain constant. Flow rate between  $P_T$  and  $P_E$  cannot be compared with the measured flow rates.

Only two pressure drops were available for comparison with measured flow rates:  $P_E - P_{A/B}$  and  $P_{A/B} - P_F$ .

SMC®, the producer of every component used in the system, offers an online tool (22) to evaluate the overall flow parameters of a series of SMC®'s components. To evaluate the overall flow parameters, first the flow parameters of each component had to be evaluated. Many component present in the system had their flow parameters evaluated in their catalogue.

Among the components present in between the analyzable pressure drop ( $P_E - P_{A/B}$  and  $P_{A/B} - P_F$ ), component 1A and 2E did not have their flow parameters present in their catalogue. One way to evaluate the flow parameter of this component is to use the procedure described in ISO 6358: 1989.

Figure 21 presents the test setup to determine pneumatic components' flow parameter.

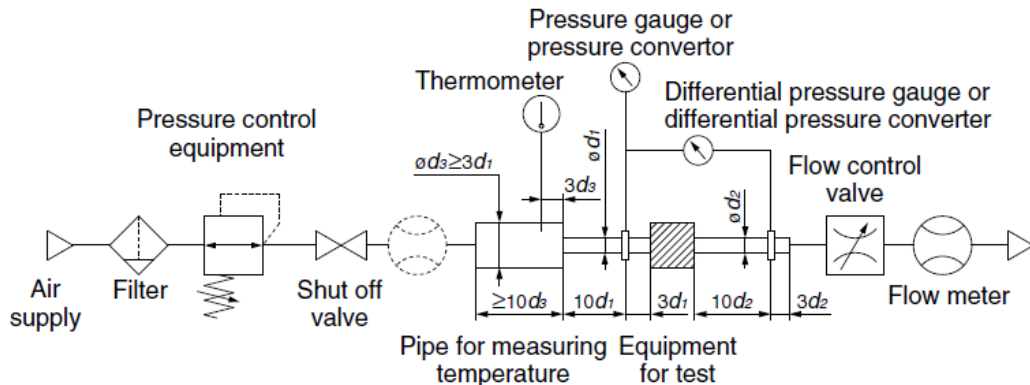


Figure 21: test circuit to determine a pneumatic components' flow parameter.

This method was attempted by substituting “equipment for test” with either component 1A and 2E, but flow rates values were too high for the sensor to read (the sensor with the maximum range was of 1000 [L/min]).

Another approach was then used. Instead that evaluating the component's parameters singularly, the component's parameters were evaluated in series with other components.

Similar components to 1A have flow parameters were present in the catalogue, while no component similar to 2E with flow parameters already estimated were available. For sake of simplicity pressure drops between  $P_{A/B} - P_F$  where not analyzed.

In practice the circuit from the output of  $Q_2$  to the inlet of actuator 1 (in the case where flow is going to chamber A) was taken as a test bench. Tests

were done using the procedure described in ISO 6358: 1989. Once flow parameters were evaluated, they were confronted with the one evaluated on SMC®'s online tool. The online tool can evaluate flow parameters when components are placed in series. Components 1A (EVHS3500-F02-X116) are dismissed, meaning that a similar component is now being produced. On the online tool all the components were placed in series, while component 1A was substituted by a more recent one from the VHS[]510 series. Once values of C and B were evaluated for both cases, then results were matched.

*Table 4: difference in flow parameters calculation.*

<b>Q<sub>2</sub> flow rate directed to chamber A of actuator 1</b>	<b>B</b>	<b>C</b>
<b>Result obtained using the standard</b>	0,15	1,81
<b>Result obtained though SMC®'s online tool using VHS2510-[]02[]-[]-[]-[]</b>	0,13	1,510
<b>Result obtained though SMC®'s online tool using VHS3510-[]02[]-[]-[]-[]</b>	0.12	1,716

Table 4 shows the valve parameters identified for valve 1A. Results obtained with VHS3510-[]02[]-[]-[]-[] are more consistent with the one measured. Parameters from VHS3510-[]02[]-[]-[]-[] were considered the same as for EVHS3500-F02-X116.

Now all parameters in the system are known. Flow parameters can be evaluated for every part of the system experiencing a pressure drop. Calculation was then repeated for circuits.

*Table 5* shows the flow parameter values for supplying chambers A and B.

*Table 5: flow parameters values.*

	<b>Supply A</b>	<b>Supply B</b>
<b>C</b>	1,716	1,729
<b>B</b>	0,12	0,12

Knowing pressure values and flow parameters, Q<sub>2</sub> can be calculated and compared with the measured flow rates values. *Figure 22* introduces the measured, calculated flow rate values and variables related to piston motion.

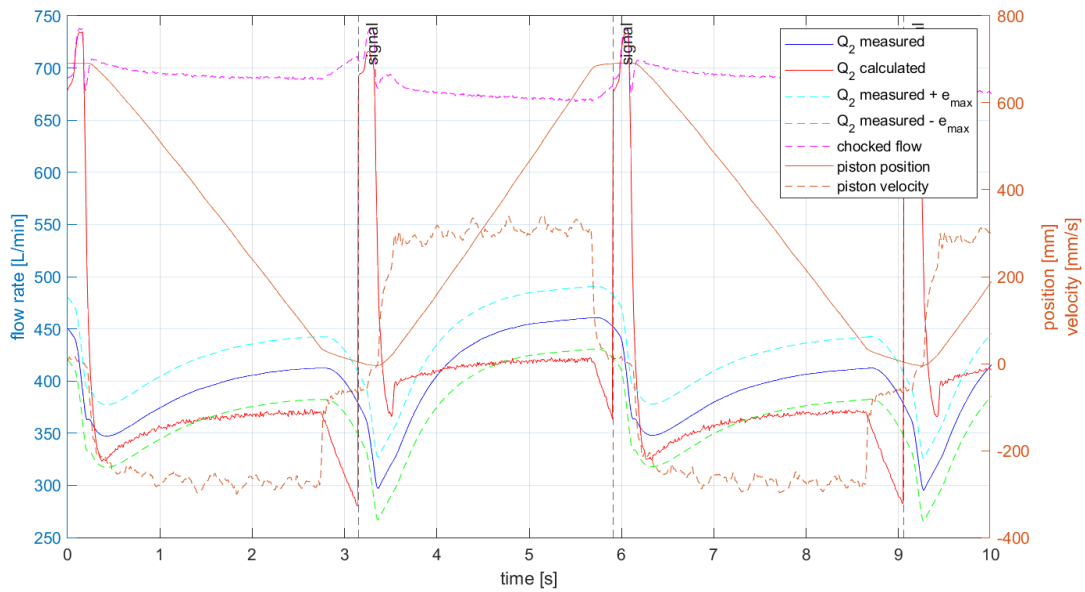


Figure 22:  $Q_2$  calculations without PESU.

Plots *Figure 22* shows the comparison between calculated flow rate and the measured one. For the pressure drops to be said consistent with volumetric flow rates values, calculated volumetric flow rates' plot must be found in the acceptable error range (between the upper and lower measuring error).

Calculated volumetric flow rates are somewhat consistent in *Figure 22*. Volumetric flow rate has the same behavior as the measured one.

Calculated volumetric flow rate is not found in the error range for most of the duration of the stroke. This is valid for both strokes. It is then evident that flow parameters are not accurately representing flow rate values in the system.

It is important to note that flow rate never reaches the choking value. This means that the decrease of flow rate with PESU is not due by geometrical restrictions.

Calculated volumetric flow rate is not consistent at stroke's beginning. In this part of the graph, called transient, calculated flow does not show the same behavior as the flow rate values from the sensor. Instead of decreasing, the flow rate increases.

This behavior occurs when the position sensor reaches the end stroke reading. When such a position is reached, a signal is sent to the DCV to move the piston in the opposite direction. DCV actuates and the flow direction is reversed. The model used to calculate the flow rates does not consider the behavior caused by the changing in flow direction.

Reasons for different transient behavior can be multiple. Two aspect must be analyzed. Factor dependent on sensors or actuators specifics (like delay of the valve or in sensor dynamics).

First factor dependent on sensors and actuators are analyzed.

To start the flow sensor dynamics are considered. Flow rate sensor dynamics are known (described in chapter 3.1.4). To consider sensor dynamics the calculated flow rate is multiplied by the Laplace transform calculated in in chapter 3.1.4. *Figure 23* shows results of *Figure 22* taking in consideration sensor dynamics.

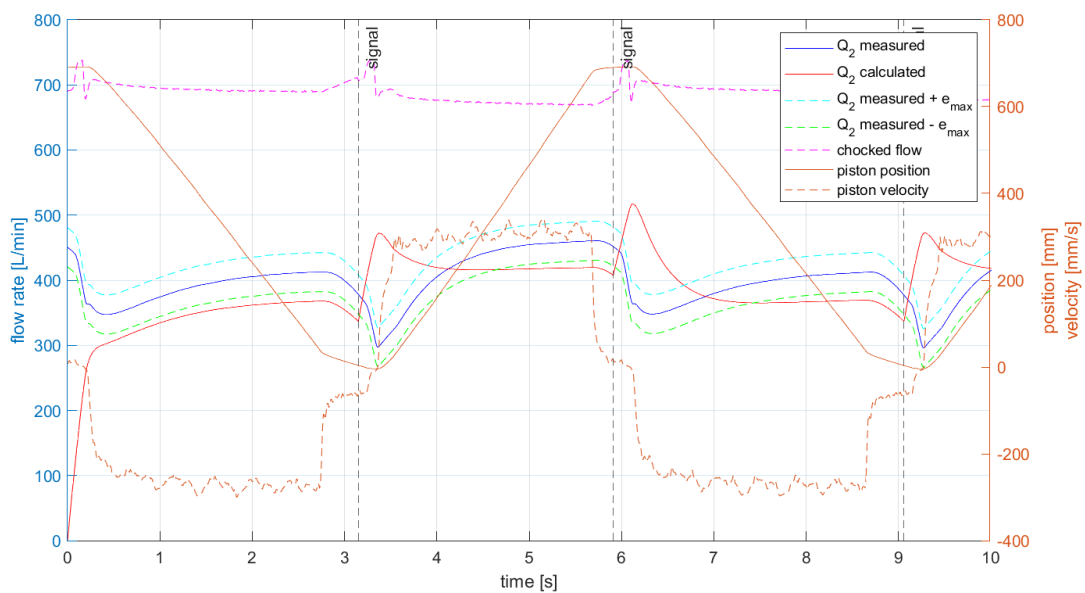


*Figure 23: calculate flow rate taking in consideration volumetric flow rate sensor delay.*

Volumetric flow rates and transient are more consistent with the measure volumetric flow rates. Still transients are not consistent. Factor dependent on sensors and actuators are then analyzed.

Let's now take in consideration factors dependent on actuators specific.

When the flow rate is changing direction, the fluid undergoes two steps. For sake of an easy explanation, the first half cycle showed in *Figure 26* (chamber B supply and chamber A exhaust) is taken as an example.

Firstly, when the solenoid is activated, the actuator does not reach zero velocity conditions. Chamber B is being supplied and chamber A acts as the exhaust. When signal is given, chamber A is supposed to act as the supplied side, while chamber B is supposed to act like the exhaust side. The piston's velocity should reach zero value and then positive value. Instead, for a brief time range negative velocity are recorded. This happens because of DCV's

delay. DCV's delay allows flow being supplied to chamber B even after signal is given to the valve.

Secondly, when the actuator is close to the cylinder's end, piston's cushions are activated (their working principle is explained in chapter o). This changes the maximum air flux to the actuator.

To account DCV's delay, it was added a small delay to the model. Before the model changes values of  $P_2$ , a delay of 70 ms (the valve delay is 64 ms but the sampling period is 10 ms) was added. This way, even though signal is given and  $P_2$  is supposed to change value,  $P_2$  remains as the previous value for the whole duration of the test. In the case of the previous example before signal is given  $P_2=P_B$ . The first time-step after signal is given, if the model had no valve delay, then  $P_2=P_A$ . Instead with the valve delay,  $P_2=P_B$  for 70 ms (seven time- steps) after signal is given. In *Figure 24* the DCV delay is taken in consideration.

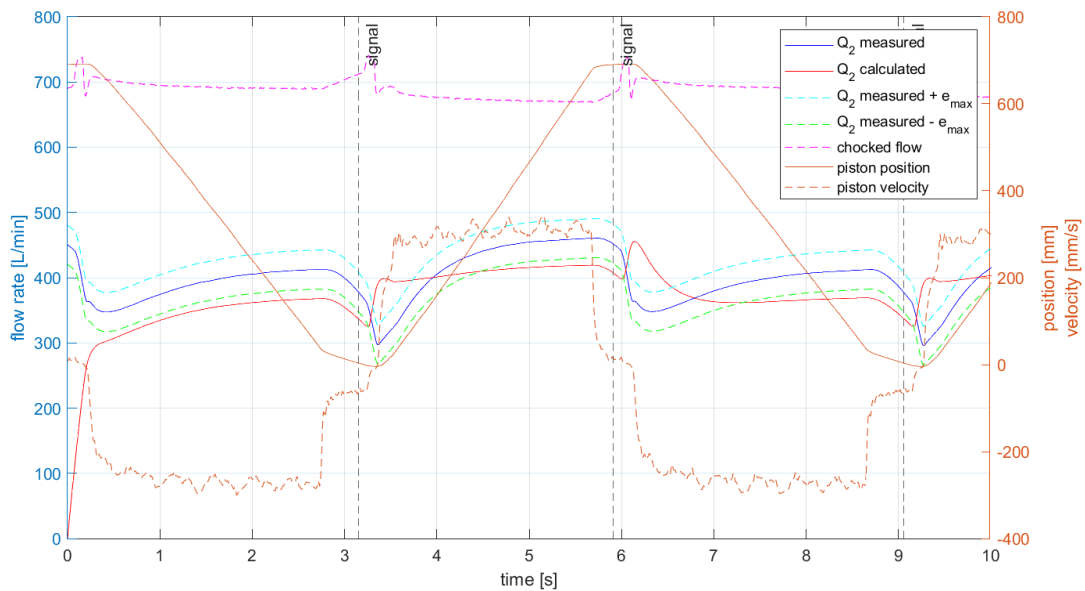


*Figure 24:  $Q_2$  calculations with PESU with valve delay.*

Comparing *Figure 23*, *Figure 22* and *Figure 24* the valve's delay reduces the transient, but it does not get rid of it. The transient takes place over a time interval of about 180 ms (*Figure 44*), while the valve has a delay of 64 ms. The valve's delay is not the main reason of different transient behavior.

*Figure 25* and *Figure 26* show velocity and pressure plots representing the cylinder's direction change transient. *Figure 25* focuses on the second transient of *Figure 24* and *Figure 22*.

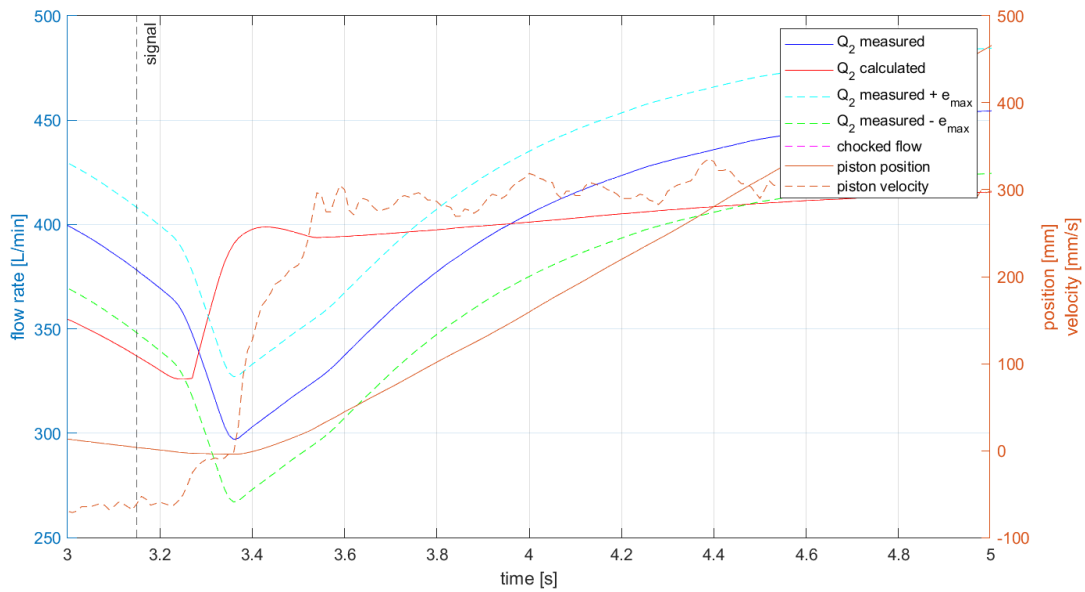


Figure 25: velocity plots over position and flow rates plots.

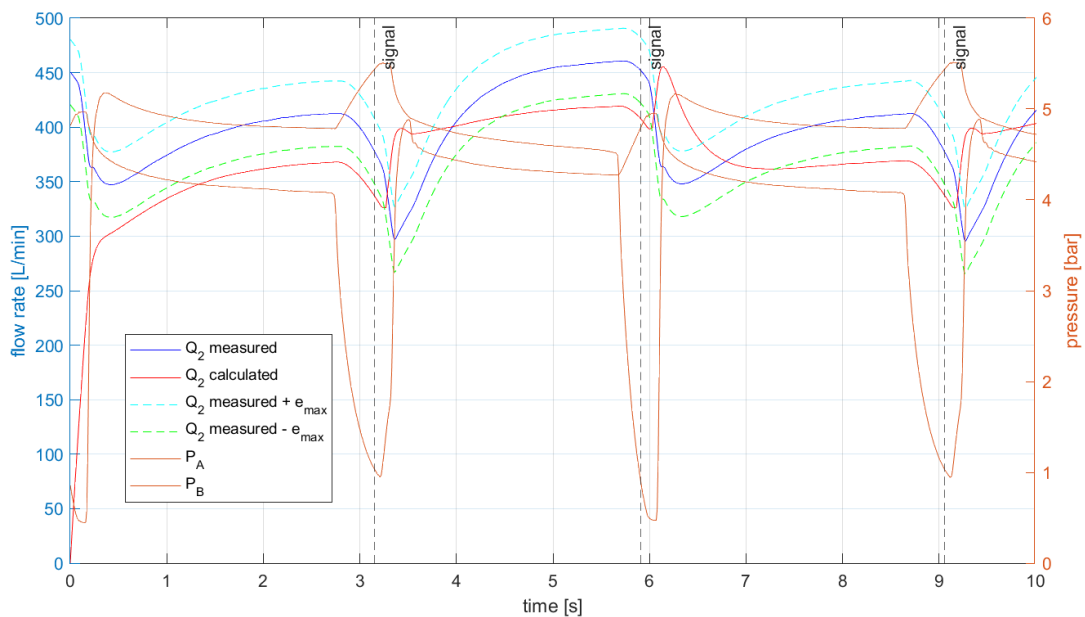


Figure 26: pressure plot over position plots.

In *Figure 25* it is shown that, once the directional control valve has reached its position, piston velocity drops to zero. This means that CA is being supplied to chamber A. This is further proven by the increase of  $P_A$  values (*Figure 26*). The reason why the transient does not match the measured values is because of the piston's cushion.

From the piston's speed decrease recorded before the first signal (time mark at around 3 seconds in *Figure 24*) it is known that the piston's cushion had been activated in the previous half cycle. Pressure in the exhaust chamber (chamber A) is higher than the measured ones. Additionally, flow param-

ters changed. Given that parameters  $C$ ,  $B$  and  $P_2$  are unknown in the case where piston's cushions are activated, an accurate volumetric flow rate estimation cannot be done. The transient cannot be estimated.

In conclusion, given the lack of data concerning the used components and the impossibility to measured pressure values inside the actuators chambers, measured pressure drops cannot be said to correctly represent measured volumetric flow rates. Although they can be said to be consistent with measured volumetric flow rates because the volumetric flow behavior is similar to the calculated one and because the calculated values are not too different from the measured one.

## 7 Results

Results from test 0 are not shown. In test 0 the team decided to have actuators going at velocities with and without PESU. To achieve that, a speed control valve (component 8 in *Figure 4*) was mounted in the system. Component 8 was mounted as such it would throttle actuators' exhaust flow rate. Throttling was applied only when PESU was not applied to the system. By throttling the exhaust flow rate, the team was able to create a back pressure which substituted the back pressure generated by PESU.

In tests 1, 2, and 3 no throttle was applied to the actuators (just on the grippers). Given that experiments were done with two different set ups, comparing results between test 0 and other tests was not done.

To evaluate the effectiveness of the unit on a pneumatic system, productivity and total energy consumption analysis were done. These parameters help indicating whenever the unit is worth investing on.

### 7.1 Total energy consumption

Total energy consumption is difficult to address without compressor's electric power measurements. To properly evaluate energy consumption of the system it would be needed to evaluate compressor's power consumption. In the case of the tested system many compressor's data would be needed to evaluate power consumption. First it would be needed the flow rate outputted by the compressor and its pressure value. On top efficiency of the compressor and efficiency of compressor's electric motor would also be needed. Oil and vapor content can be neglected.

Although flow rates and inlet pressure values are known, compressor's efficiency and electric motor's efficiency were not available. The writer reminds that to test the systems a proper compressor was not available.

To evaluate the total amount of energy used by the system, the inlet power to the system was integrated over the whole duration of the experiments.

The inlet power can be evaluated as:

$$W_{in} = Q_{in} \cdot P_{in} \quad (22)$$

The CA entering the system can be considering as source of the inlet power. Integrating equation (22), over the whole recorded time range, the total amount of used energy can be estimated.

$$E_{in} = \int_{t_0}^{t_f} W_{in} dt = \int_{t_0}^{t_f} (Q_{in} \cdot p_{in}) dt \quad (23)$$

In page 32 air is considered as an ideal fluid. Applying equation (8) to equation (23).

$$\begin{aligned} \int_{t_0}^{t_f} (Q_{in} \cdot p_{in}) dt &= \int_{t_0}^{t_f} (Q_{in} \cdot \rho_{in} \cdot RT) dt = RT \int_{t_0}^{t_f} (Q_{in} \cdot \rho_{in}) dt \\ &= m_{in} \cdot RT \end{aligned} \quad (24)$$

$m_{in}$  being the total CA entering the system and is equal to  $m_{in} = Q_1 \cdot \rho_0 \cdot T$  being the fluid temperature which is constant and is assumed at 25°C or 298 K.

## 7.2 Time cycles

In industry processes speed is the most important factor. Pneumatics is widely used in production plants with high level of automation. Production plants are usually organized in production line in which the takt time of each station (time taken for each station to fully complete its task on the product) is strictly related to the rate at which finished products leave the line. In theory the longest takt time is equivalent to the rate of finished product delivery.

In tests a cycle is defined as the time it takes for the actuator to go back in the starting position. To evaluate how the unit affects system's cycle time, the number of cycles is counted and divided by the time duration of the test. Cycles' mean velocity is then given.

## 7.3 Energy consumption per cycle

Total energy consumption does not give any information about the relative energy consumption needed to accomplish the same action. The amount of energy that the system needs to complete one cycle with and without PESU must be evaluated to assess PESU effectiveness.

The relative consumption of a cycle in each experiment is given as a mean of the total amount of energy used by the system divided by the total number of cycles done in the same time interval. Results are shown in *Table 6*.

## 7.4 Data results

Each experiment was done once. The results shown are data coming from analyzing one recording. Inlet conditions were kept constant in all experiments. Every pressure regulator and throttle valve had the same set up in all experiments. Results of the experiments are reported in Table 6.

*Table 6: experiment's results.*

	Test 1		Test 2		Test 3	
	With PESU	Without PESU	With PESU	Without PESU	With PESU	Without PESU
<b>Total C.A. consumption at atmospheric pressure (J)</b>	45 379	84 103	42 274	82 645	13 851	24 724
<b>Average cycle speed (seconds/cycles)</b>	6.79	5.91	8.04	6.49	0.54	0.49
<b>Consumption of C.A. per cycle (J/cycle)</b>	2 521	4 102	2 818	4 467	61.84	100.10

## 8 Results analysis

The following chapters give a detailed explanation of changings in the system variables. To provide the reader with a better understanding of what is happening in the system, flow rates and pressure values are analyzed independently.

Results show that experiments' variables had the same behavior in different tests. In all tests, when PESU was applied, cycle time increased while energy consumption decreased. All tests can be then said to give consistent results. To avoid purposeless repetitions, just plots of test 1's parameters are shown. Test 1, having one actuator with a position sensors, is the only test where all data are known. Other tests had one actuator without position sensors (actuators 3 and 4 are controlled via reed sensors).

### 8.1 Mass flow rates behavior

In *Figure 27* mass flow rates from flow rate sensors in test1's experiments are compared.

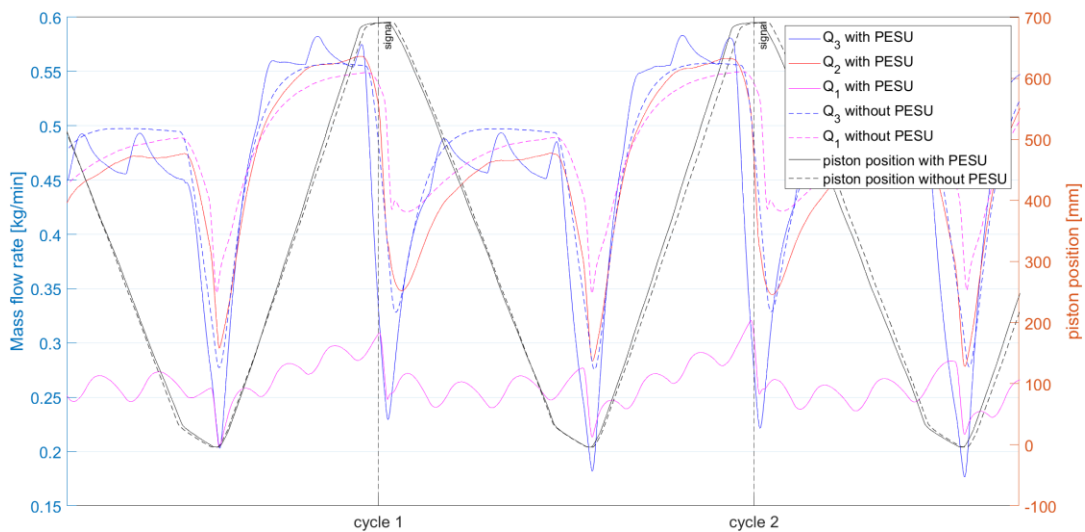


*Figure 27: comparing flow rates in test 1<sup>3</sup>.*

In *Figure 27* it shown that  $Q_2$  and  $Q_3$  are not always lower when PESU is used. This can be consistent with results. Data from *Table 6* show that pis-

---

<sup>3</sup> The graph above is used to compare cycle behaviour in both experiments. The time axis (x-axis) is not equal for plots with and without PESU. Cycle with PESU takes more time to be completed. Cycles with PESU are showed with their time variable multiply by a factor which corresponds to the ratio of time taken for the two experiments to complete 1.5 cycle. This way, the two cycle are compared.

ton's velocity is lower in the case where PESU is present. Volumetric flow rate is dependent on the actuator speed (equation (10) and (11)), but mass flow rate values are not found to be lower when PESU is applied (*Figure 27*). From equation (9) mass flow rate is dependent both on the pressure of the fluid and volumetric flow (other parameters are supposed to be constant). A reduction in volumetric flow, if pressure is increasing, does not mean a reduction in mass flow rate.

To verify that measured volumetric flow rates are lower when PESU is applied, flow rates must show as if they were recorded at their relative pressure (actual volumetric flow rates) and not at gauge pressure.

By doing the following calculation the actual volumetric flow rates can be obtained:

$$Q_1 = Q_1 \cdot \frac{P_0}{R \cdot T_0} \frac{R \cdot T^*}{(P_E + P_0)} \quad (25) \quad Q_2 = Q_2 \cdot \frac{P_0}{R \cdot T_0} \frac{R \cdot T^*}{(P_C + P_0)} \quad (26)$$

$$Q_3 = Q_3 \cdot \frac{P_0}{R \cdot T_0} \frac{R \cdot T^*}{(P_F + P_0)} \quad (27)$$

It can be obtained the real volumetric flow rates, which are plotted in *Figure 28*.

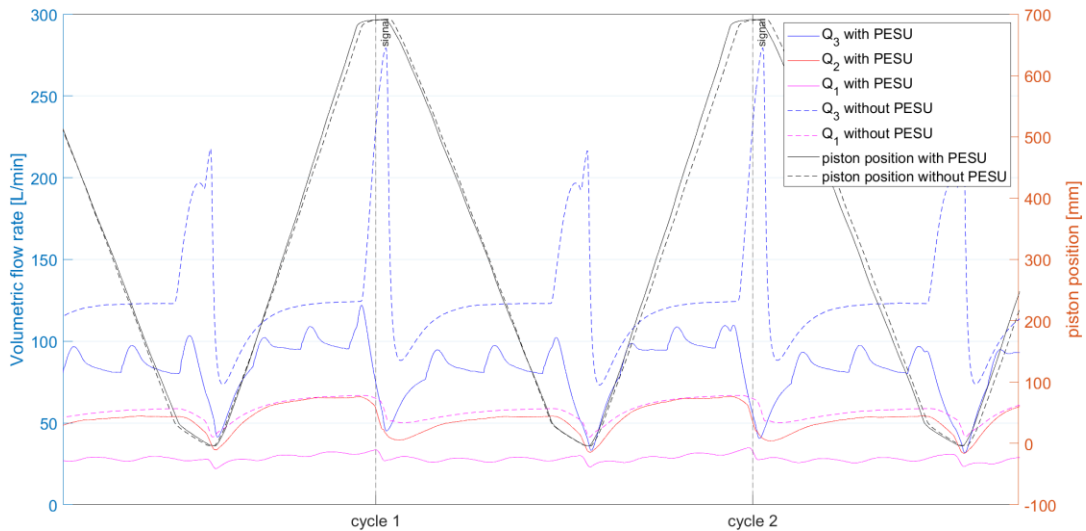


*Figure 28: real volumetric flow rate in test 1's experiments<sup>3</sup>.*

From *Figure 28* it can be seen how supply mass flow rate (magenta lines) is much smaller when PESU is applied. This is coherent with results from *Table 6*.

## 8.2 Pressure in the actuators

In *Figure 29* actuator pressure values are plotted in relation to piston's position.

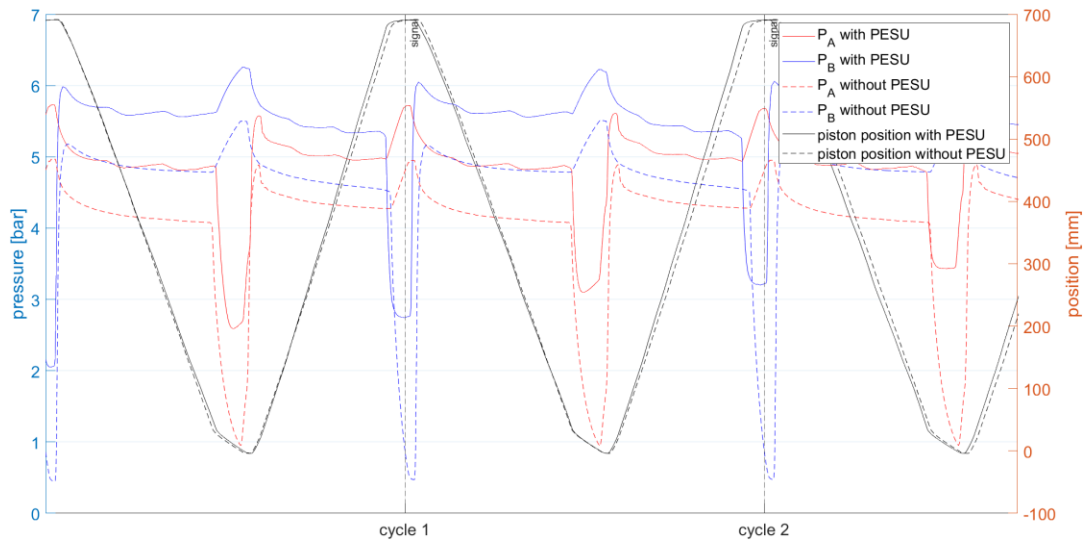


*Figure 29: pressure plot in actuator 1 in test 1<sup>3,4</sup>.*

Since it was not possible to sample pressure values inside the actuator's chambers, pressure values are sampled immediately outside the actuator input and exhaust port.

The recorded pressure values are reported in *Figure 29*. By comparing the different pressure plots in *Figure 29* it is clear how pressure lines  $P_A$  and  $P_B$  have higher values when PESU is used. In general, pressure values when PESU is applied are approximately 1 bar higher than when PESU is not applied. No throttling was applied in both experiments. The only difference between the experiments is PESU. These results indicate that PESU increases backpressure value in the actuator. *Table 7* reports the minimum chamber pressure values recorded in each experiment.

*Table 7: minimum flow rate values<sup>4</sup>.*

	With PESU		Without PESU	
	$P_A$	$P_B$	$P_A$	$P_B$
Min recorded pressure values [Bar]	2,54	2,05	0,94	0,45

<sup>4</sup> At gauge pressure

In conclusion, for the same piston's position, end stroke pressure values are higher when PESU is applied. This is also valid for both  $P_A$  and  $P_B$  and in every end stroke position of tests.

The increase of backpressures can be verified both graphically (from *Figure 29*) and from *Table 7* (where the lowest recorded value for pressure over the whole sampled time are reported). It can then be stated that the unit causes back pressure at the exhaust.

It is important to notice the behavior of pressure value at the end stroke. For example, in the first cycle shown in the piston is moving to its zero position (zero values for the position sensor). In this case CA is being supplied to  $P_B$  and CA is being exhausted from  $P_A$ . When the piston approaches the end stroke position, pressure  $P_A$  decreases, while  $P_B$  increases. This behavior is due to piston's cushions. *Figure 30* shows pressure in the chambers over piston movement when PESU is not applied.

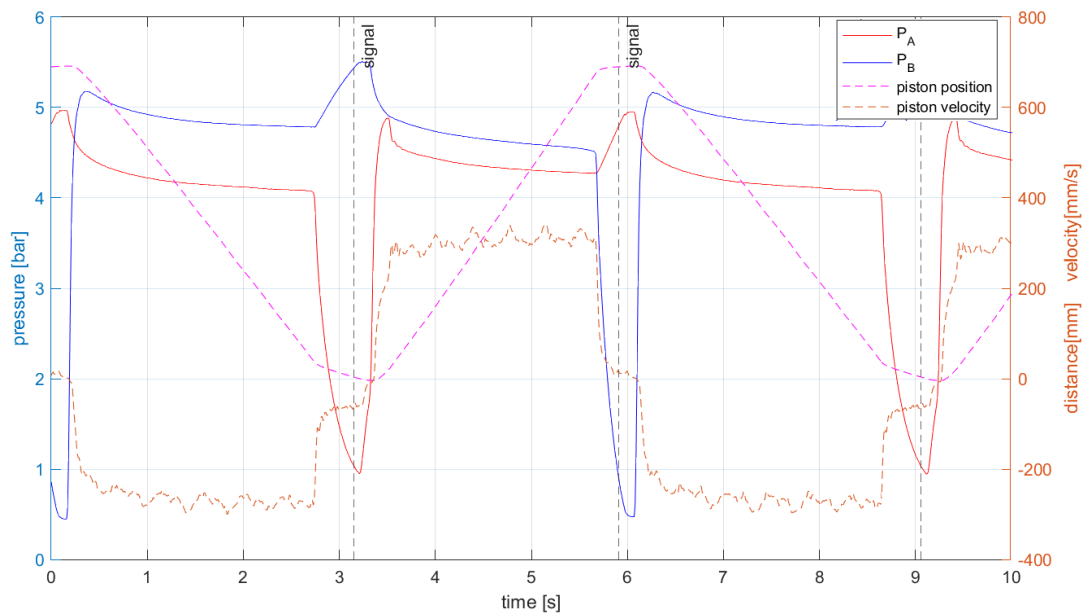


*Figure 30: pressure values without PESU over piston's velocity and position<sup>4</sup>.*

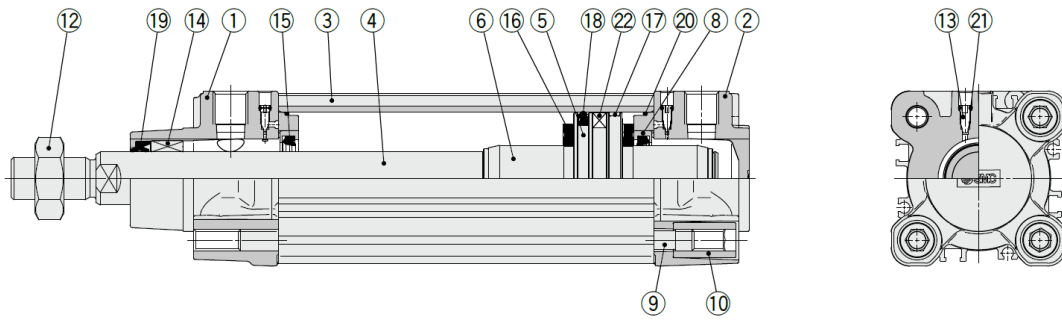


Figure 31: actuator 1 cross section.

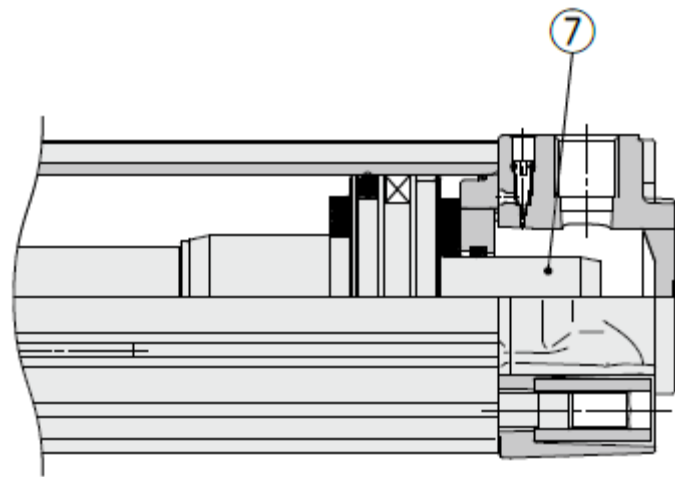


Figure 32: focus on actuator 1 cushion ring.

When the piston is close the cylinder end, the cushioning system is activated.

If the piston is moving toward the zero position (i.e., the piston is retracting), cushion ring A (component 7 in *Figure 32*) enters the cushion seal (component 8 in *Figure 31*). CA, which normally flow through the cushion seal is forced to flow through cushion valve (component 13 in *Figure 31*). Cushion valve is a much smaller orifice than the cushion seal. Pressure in chamber A (different from  $P_A$ ) increases, exhaust flow rate decreases and speed decreases. Given the lower velocity, also  $P_B$  increase and the supply flow rate decreases.

In *Figure 30*  $P_A$  decreases instead of increasing. This happens because Chamber A's pressure is sampled outside the cylinder, it does not report the pressure in between dumper (component 16 in *Figure 31*) and the cushion seal, which is the pressure values that influence the dynamics of the actuators. Flow rates being exhausted from actuator 1 are so small that the pressure drop between  $P_A$  and  $P_F$  is not large and decreases (*Figure 45*). Act<sub>1</sub> contains cushion on both sides. The same behavior is experienced by  $P_B$  when the piston is reaching the full-length position.

### 8.3 Pressure values before at the supply and at the exhaust

The supply and exhaust pressures with and without PESU are presented in *Figure 33*. In both cases:  $P_C$  is the CA's pressure supplied to the valve, while  $P_F$  is the CA's pressure at the exhaust. When PESU is not applied,  $P_C$  acts as the external supply and as the supply to valves, so in this case  $P_C = P_E$ .

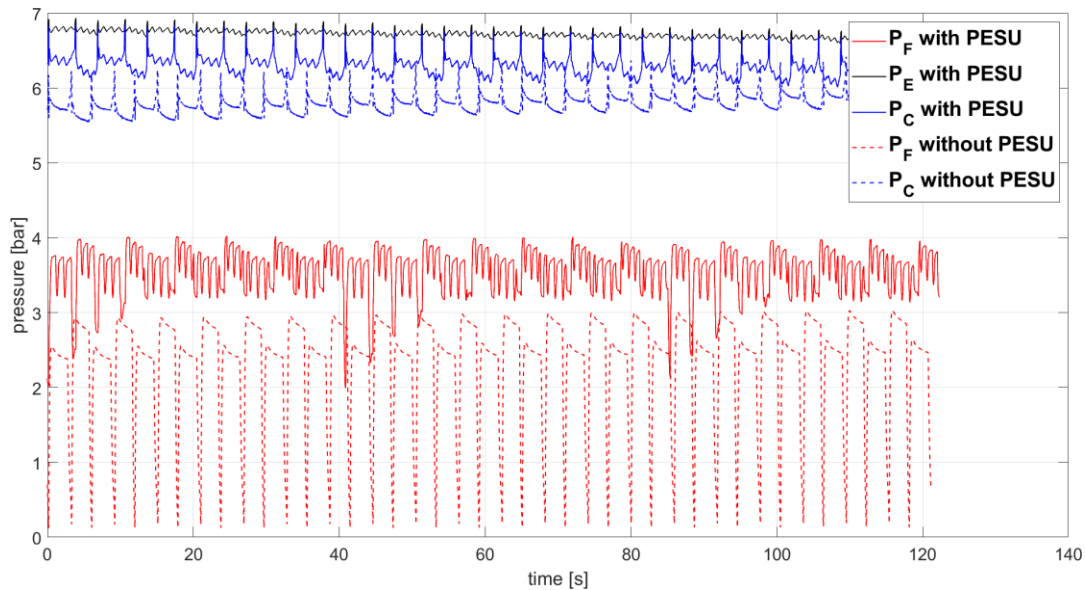


*Figure 33: pressures value in test 1's experiments<sup>4</sup>.*

As a farther proof of what was stated in chapter 8.2: in the case PESU is not used, exhaust pressures reach lower pressure values than when PESU is applied. For instance, when PESU is applied, exhaust pressure never reaches values lower than 2 Bar<sup>4</sup>. While when PESU is not applied, exhaust air's pressure reaches lower values, close to zero<sup>4</sup>.

Supplied pressure values ( $P_C$ ) to actuator 1 have higher values when PESU is applied. These are approximately 1 bar higher when the unit is applied. When PESU is applied both the pressure supplied to the valve ( $P_C$ ) and the pressure coming from the external supply are higher ( $P_F$ ).

The higher-pressure values supplied to the valve are due to air recirculation. PESU's working principle is to recirculate air from the exhaust. The booster used in PESU has a pressure ratio of 2, meaning that booster CA output pressure is double with the respect to the inlet one. The exhaust pressure fluctuates around 3.5 Bar<sup>4</sup>, double of which is 7 Bar<sup>4</sup>, which is higher than CA's pressure values from the external supply ( $P_F$  fluctuates around 6.8 Bar<sup>4</sup>). It is then expected that, when PESU is applied, supplied air to DCV ( $P_C$ ) has higher pressure levels than when PESU is not applied.

It was also recorded that CA's pressure values from the external supply are higher when PESU is applied (straight  $P_E$  line in *Figure 33*) than pressure

values from the external supply when PESU is not used (dashed  $P_C$  line in *Figure 33* where  $P_C = P_E$ ). CA is supplied to the system with the same external supply. Plus, two pressure regulators ensure that pressure value is identical in both experiments.

The reason for external supply pressure values to be higher in the case where PESU is applied is the presence of check valves in the unit. At first the external supply is powering the system. As time passes and PESU recirculates air, repressurized air increase its pressure value over  $P_E$ . The valve that allows  $Q_1$  to supply the system closes to allow repressurized CA to supply the system. In this instant  $Q_1$  increases  $P_E$ . Once  $P_E$  reaches pressure values higher than the repressurized air, the valve that allows  $Q_1$  to supply the system opens and the external supply is supplying again the system. This happens until repressurized air is lower than  $P_E$ . Once this happens the cycle repeats. The alternation between external supply and repressurized air acting as supply for the system increase  $P_E$  to a certain value. The increase in  $P_E$  explains the decrease in  $Q_1$ . A similar explanation is used to describe the unsteady behaviour of  $P_E$  in chapter 8.5.

In *Figure 34* the process of repressurized CA substituting the main supply as CA source to the actuators can be seen.

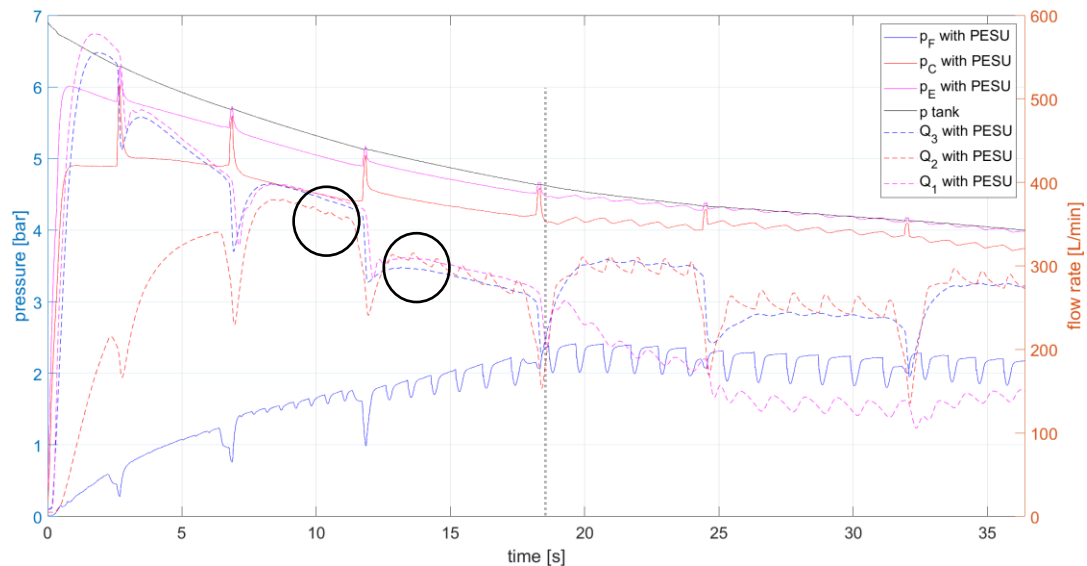


*Figure 34: flow rate plots over pressure plots in test 0.2<sup>4</sup>.*

At first the supply flow rate from external source ( $Q_1$ ) has approximately the same values of  $Q_3$ . Once PESU re-pressurized CA has reached pressure values higher than  $P_E$  and re-pressurized air acts as supply, some spiked in  $Q_2$  can be seen (marked by black circles). At the same time tank pressure is decreasing.  $P_E$  is decreasing as well and  $Q_1$  is decreasing. Around 18 seconds

(marked by the dotted black line)  $Q_1$  undergoes a sudden decrease and the system is mainly powered by the recirculated CA.

In *Figure 33* pressure values  $P_C$  using PESU and not using PESU are converging because  $P_C$  using PESU is decreasing. This is due to a decrease in tank pressure values. It must be estimated if tank pressure is diminishing due to a decrease on external supply performance or the system is using CA at a too high rate.

## 8.4 Causes of speed reduction

Data show that when PESU is applied to the system, the actuator's speed is reduced. This is farther proven by the reduction in flow rates.

Data also show that backpressure is generated at the exhaust. Furthermore, supply CA's pressure levels to the actuators are higher when PESU is applied. Knowing these an explanation of actuator speed reduction can be given.

Let's first start to what the system experiences. At first the system is supplied with CA. Air is free to circulate in the system. Once air is supplied to the actuators, the piston accelerates until pressure difference is fixed and force balance is found. The piston now has a constant velocity. Recalling that:

$$F = m \cdot \ddot{x} + F_v + F_{ext} = P_A \cdot A_A - P_B \cdot A_B \quad (28)$$

If forces in the piston are equal to zero during movement (neglecting seal friction which is dependent on velocity and external forces), then  $P_B$  and  $P_A$  must balance each other, then  $P_A \cdot (A_A/A_B) = P_B$  ( $A_A/A_B$  is always greater than one).

Let's suppose that PESU is not being applied and pressure is supplied to chamber B, the piston is moving in the negative direction. When the piston will reach a steady velocity state,  $P_B$  will be equal to  $P_A(A_A/A_B)$ , where  $P_A$  is given by pressure drop that air experiences to win circuit resistance. If circuit resistance is increased, then also  $P_A$  will increase. To reach steady velocity state,  $P_B$  will increase as well. Recalling that the ratio  $(P_B+P_o)/(P_C+P_o)$  proportionally determines the amount of flow rate to the actuators. If  $P_C$  remains constant and  $P_B$  increases, then the flow rate will decrease. Knowing that the piston's speed is proportional to the supply flow rate, a decrease of flow rate means a reduction in piston's speed.

When PESU is applied to the system, the back pressure at the exhaust is increased. Taking as an example the case described in the previous paragraph, inserting PESU in a system means that the exhaust pressure  $P_A$

is increased.  $P_B$  is hence increased as well (to maintain the pressure balance in the cylinder). It must be recalled that PESU increases  $P_C$  pressure values. Given that  $Q_2$  is dependent on  $P_C$ , an increase in  $P_C$  corresponds to an increase of  $Q_2$ . Also, an increase of  $P_C$  lowers the pressure ratio. To evaluate the effect of back pressure and supply pressure increase, a proper comparison between the two theoretical flow rates must be done. The calculated flow rates ( $Q_2$ ), pressure ratios, and piston velocities and piston acceleration are presented in Figure 35 and Figure 36.

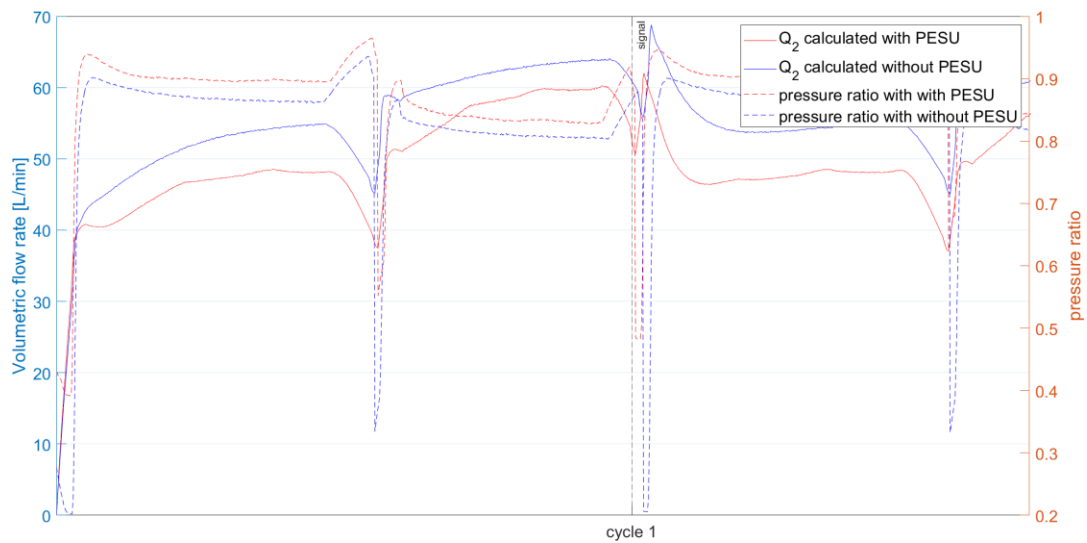


Figure 35: calculated volumetric flow rates and pressure ratio comparison<sup>3</sup>.

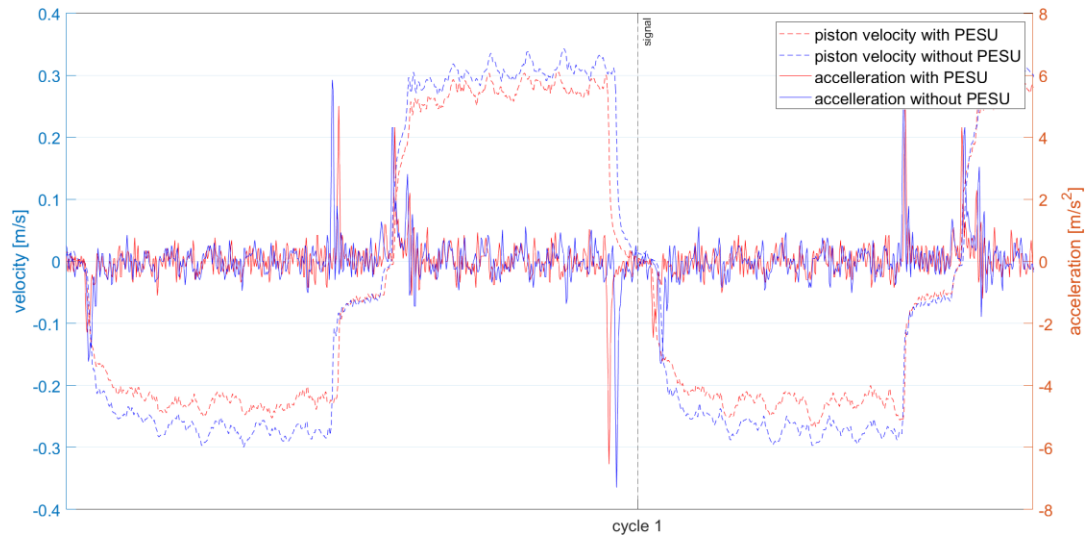


Figure 36: velocity plot over acceleration plots<sup>3</sup>.

As shown in *Figure 36*<sup>3</sup>, velocity and acceleration<sup>5</sup> are always lower in magnitude in the case when PESU is applied (blue line is always greater in magnitude with respect to the red line). In *Figure 35* it is shown that pressure ratio is smaller when PESU is not applied.

Speed is proportional to volumetric flow rate which is smaller when pressure ratio is higher. Results from *Figure 35* and *Figure 36* are consistent with this statement. In *Figure 35* pressure ratio is always higher when PESU is applied. Calculated volumetric flow rate with PESU is always smaller than calculated flow rate without PESU.

## 8.5 Sudden rises in flow rate when the unit is applied

When PESU is applied, some sudden increase in flow rates values were recorded. This behavior can be identified by the spike in  $Q_1$  and  $Q_3$  (shown with a dark orange ring in *Figure 37*). This sudden increase can be seen also in pressure values (*Figure 33*).

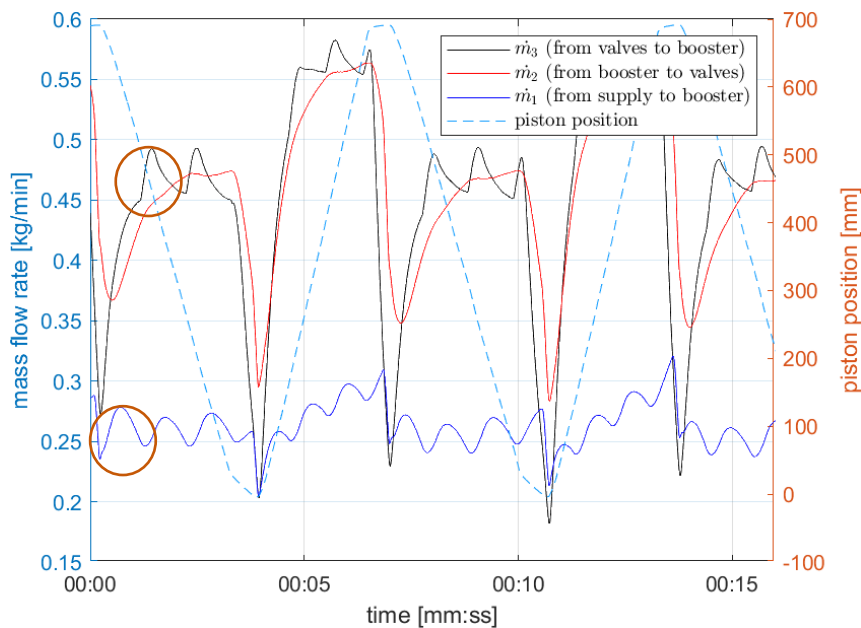


*Figure 37: flow rates with PESU.*

The cause for such behavior is caused by the working principle of the unit. As explained in chapter 2, the actuator supply air comes from two different sources. One is from the main supply; the other is from re-pressurized exhaust air. The two CA source do not supply the actuators simultaneously.

<sup>5</sup> Acceleration is obtained by integrating velocity values using an open-source first order finite-difference method MATLAB code (19).

Re-pressurized exhaust air is supplying the actuators only if its pressure values are higher than the pressure values from the main supply and in the DCV's inlet line (because of the pressure regulator). At first the actuators are supplied with flow rate coming exclusively from the external supply. Once re-pressurized exhaust air reaches a pressure value higher than the pressure value from the main supply, then the re-pressurized exhaust air acts like a supply.

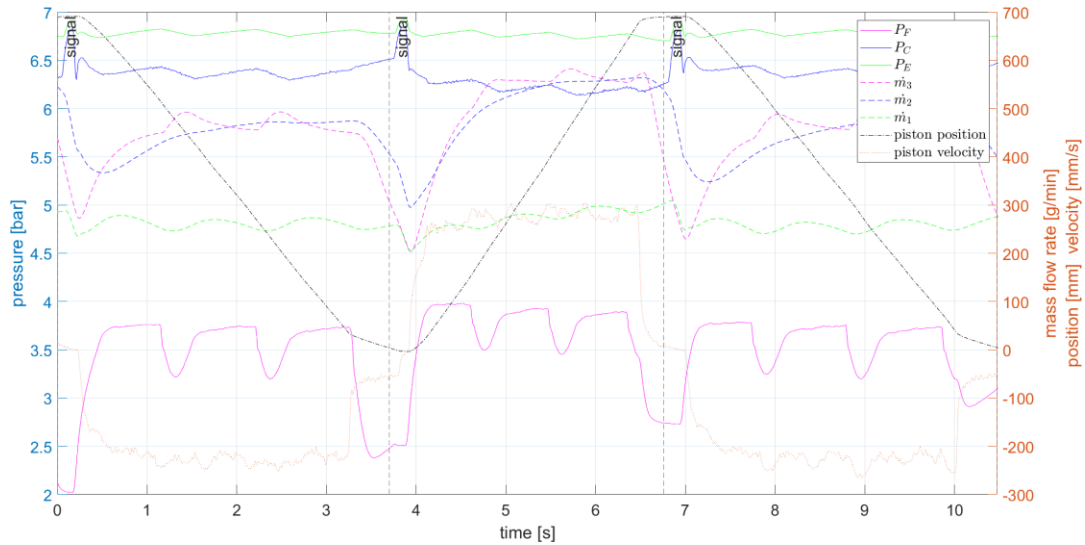


Figure 38: pressure to valve over volumetric flow rates<sup>4</sup>.

From Figure 38 the changes of fluid variables can be seen.  $\dot{m}_2$  has a steady behavior, while  $P_C$  shows some sudden increase in pressure values. Increases in  $P_C$  are consistent with increase in  $P_E$ .

When  $P_C$  and  $P_E$  record pressure increase, the system is supplied with recirculated air, the flow from external supply is closed while the one from air recirculation is opened. Increased  $P_C$  values are due to the higher pressure from recirculated air. On the other hand,  $P_E$  increase is due to cease air supply from the tank, i.e.,  $P_E$  and  $P_T$  are reaching the same value.

Mass flow rates  $\dot{m}_1$  and  $\dot{m}_3$  do show this behavior with certain delay (due to the flow rate sensors' delay). At first, exhaust air pressure ( $P_F$ ) is constant, meaning that exhaust air is being recirculated. When recirculated air acts as a supply, air pressure value in pipeline 13 of Figure 2 drops. Meanwhile, the booster continuously supplies the unit with repressurized air. Once pressure in pipeline 13 drops to pressure level lower than  $P_C$ , recirculated air does no more supply the system. Sometime in between the time span when recirculated air acts as system supply, exhaust pressure drops. When supply pressure drops,  $\dot{m}_3$  increases. So, when PESU is recirculating, exhaust flow rate increases.

The opposite happens for  $\dot{m}_1$ . When the system is recirculating air,  $P_C$  increases and the pressure ratio  $P_C/P_T$  increases. As shown in equations (20)

and (21) volumetric flow rate values are indirectly proportional to supply pressure ratio. An increase in  $P_c$  means a decrease in  $\dot{m}_1$ .

Once  $P_E$  reaches higher values, then re-circulated air pressure,  $P_E$  becomes the supply and re-circulated air is isolated from the supply.  $P_E$  pressure values are then decreasing and  $\dot{m}_1$  increases. Once recirculated air pressure increases over  $P_E$ , then the external supply no longer provides flow to the actuator and cycle repeats.

## 8.6 Supplied pressure value

Experiments in each test were done consecutively. No inlet parameter was modified. For this reason, the supply was assumed to be constant. Recording of tank pressure are consistent with this last statement with a certain range. Measured tank pressures are shown in *Figure 39*, *Figure 40* and *Figure 41*.

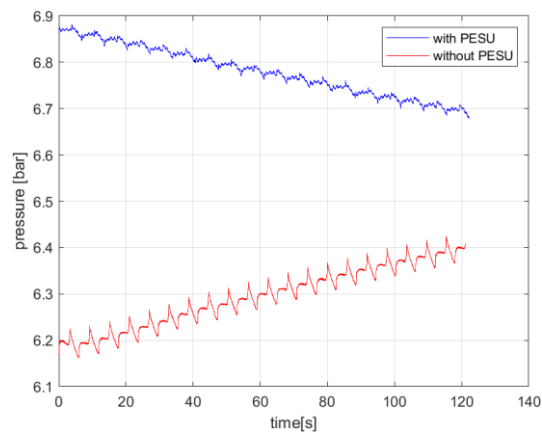


*Figure 39: tank pressure test 14.*

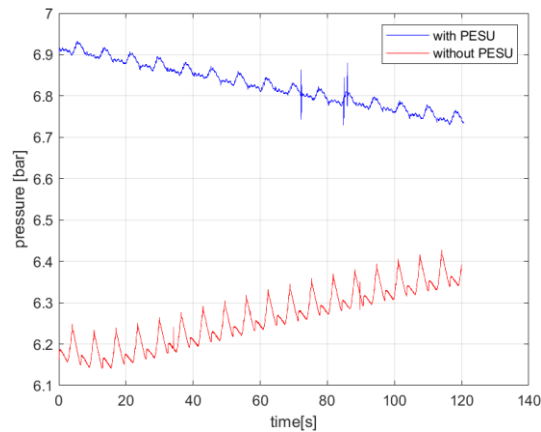


*Figure 40: tank pressure test 24.*

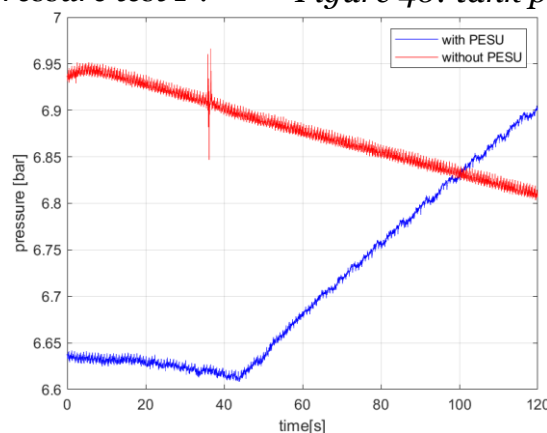


*Figure 41: tank pressure test 34.*

Tank pressure is not constant over time. *Figure 39*, *Figure 40* and *Figure 41* show that tank pressure is fluctuating over a range of 0.2 Bar.

Tank pressure behavior does not seem to be influenced by the application. It is expected that pressure will decrease and then stabilize around a specific value, but this does not happen. In *Figure 39* and *Figure 40* tank pressure values are decreasing in the case where PESU is applied and increasing where PESU is not applied. The opposite behavior is recorded in *Figure 41*: tank pressure values are increasing in the case where PESU is applied and decreasing where PESU is not applied.

An option to reduce tank pressure fluctuation could be to install higher capacity tanks, but no bigger tanks were available.

## 8.7 Temperature changes

To fully evaluate the effect of PESU on the system, also air temperature had to be taken into consideration. It was needed to evaluate how the unit affects temperature values. On each connection of the system to PESU temperature sensors were placed as the closest sensor to PESU. This way temperature readings are only dependent on the unit.

The effects of PESU on temperature are analyzed. First supply air's temperature is compared between the tests. Temperature of air coming from the external supply ( $T_1$ ) and the air going to the actuators ( $T_2$ ) are subtracted,  $T_2 - T_1$ . No temperature sensors were available at the actuator. Since  $T_3$  measured the temperature values of the exhaust air and  $T_2$  measured the temperature value of air at the actuator supply, those values were taken as reference value for air temperature's values at the actuators. Results of the subtraction  $T_2 - T_3$  are shown in *Table 8*. For sake of completeness, also difference over  $T_3 - T_1$  is given.

The greatest difference shown is the biggest in absolute value among positive and negative differences. The sign is shown to evaluate the changes in direction of temperature change. Results are shown related to the experiments where PESU is applied.

In the case where PESU is not applied, temperature sensors  $T_2$  and  $T_1$  are placed in series. Showing temperature difference between  $T_2$  and  $T_1$  would have given no information since their values is almost identical.  $T_3$  reports exhaust air temperature. Showing the difference between  $T_3$  and one between  $T_2$  and  $T_1$  would mean showing temperature increase due to the actuators, something that is not interesting. No temperature results are shown when PESU is not applied.

*Table 8: temperature max difference [ °C ] .*

	<b>Test 1</b>	<b>Test 2</b>	<b>Test 3</b>
$T_2 - T_1 = [^{\circ}\text{C}]$	1.05	1.34	-0.67
$T_2 - T_3 = [^{\circ}\text{C}]$	2.50	1.49	3.19
$T_3 - T_1 = [^{\circ}\text{C}]$	-2.37	-0.42	-3.70

In chapter 6.3 temperature is assumed to be constant at 25°C. Because in every case temperature differences are very small, smaller than 4°C (as reported in *Table 8*). Such a value is too small to influence calculations. A change of 3.70°C (maximum changes recorded) will mean a difference of 1.3% over the flow rate calculation. The temperature sensor has a total error of 1% at 25°C (23). Given that the two errors are comparable to each other and that mass flow rates are rounded to the third decimal, temperature difference can be safely ignored.

$T_3$  measures the exhaust air temperature. Thus, it measures air after the fluid has gone through all dissipative components in the system.  $T_3$  can be considered as the air temperature at the piston exhaust.  $T_2$ , which is always higher than  $T_3$  (*Figure 46*, *Figure 47* and *Figure 48*), is considered as the temperature at the inlet of the actuators. In all experiments  $T_2$  and  $T_3$  do not differ much from  $T_1$ . As shown above, even an error of 4°C won't be a problem.  $T_1$ , which has almost constant behavior, is taken as the air temperature value in the actuators. For sake of calculation simplicity, 25°C was chosen as reference temperature.

In the case of *Figure 46* and *Figure 47*, air temperature slowly increases (0.5°C/min). Temperature increase is not constant and is dependent on PESU activity. In test 3 (*Figure 48*) air temperature does not increase but decreases.

Test 1 and test 2 both use a big actuator with high flow rates. Dissipation and heat generation are closely related to flow rates.

In test 3 (*Figure 48*) dissipations and heat generation is minor. It is so low that is all released in the environment. Because environment's temperature is lower than the fluid temperature. CA's temperature is lowered.

In test 1 (*Figure 46*) and test 2 (*Figure 47*) too much heat is generated to keep the air temperature stable. Some generated heat is exchanged with the environment, some is then exchanged with the fluid, increasing air's temperature.

## 9 Data analysis

Before modifying a production plant, costs and benefits analyses must be done. The PESU is small in size, it does not represent a safety problem, it does not need any external power source other than CA and it is easy to mount. Changing PESU's setting can be considered easy since only the outlet pressure can be regulated via component 9 in Figure 2.

Understanding that placing PESU in a production plant most likely won't cause any issue, performances analysis must be evaluated. Once this is done, the economic gain of installing PESU can be evaluated.

### 9.1 Performances analysis

Evaluating efficiency is not simple because it would require input and output power to be known. While input power can be known, output power is not always known. Output power is calculated from the multiplication of the useful force developed in the actuator times its velocity. This calculation could only be done for test 1, where useful force could be evaluated from piston's acceleration and where piston's velocity is known. In test 2 and test 3 this could not be done because there is no information relative to piston velocity or acceleration.

A much simpler analysis consists of evaluating system performances. This was done by evaluating the gain of a specific quantity:

$$gain = \frac{\text{performances with the unit}}{\text{performances without the unit}} [\%] \quad (29)$$

Results displayed in *Table 9* highlight the advantages and disadvantages of PESU.

*Table 9: system gain.*

	<b>Test 1</b>	<b>Test 2</b>	<b>Test 3</b>
<b>Average cycle speed (seconds/cycles)</b>	115%	124%	110%
<b>Consumption of energy per cycle (J/cycles)</b>	61%	63%	62%

The unit was conceived to reduce energy consumption. Results in *Table 9* are consistent with this last statement. Given the same number of cycles, when the unit is applied, energy consumed by system is always lower. Results report that about 38% of energy is saved by applying PESU to the sys-

tem. Percentage of the decrease in energy consumption seems to not depend on the application.

On the other hand, changes in average cycle time seems dependent on the application. In all applications the time taken for the system to complete the same cycle increases. From results in *Table 9* it seems that the higher volumetric flow is required by the system, the higher the time cycle increase.

## 9.2 Return on investment period analysis

The economic benefits of installing the unit largely depends on the system and the plant it has been applied to.

The economic effectiveness of PESU is dependent on the time cycle increase and the energy saving must be evaluated. Since it does not exist a method to evaluate system performances analytically, performance must be evaluated experimentally.

Values for energy saving gain and cycle time gain can be obtained from results of test 2 *Table 9*. Test 2 represents an industrial CAS (a packaging system) and shows the worst performance. To evaluate PESU performance in the worst-case scenario, results from test 2 are used for the economic analysis.

The return of investment period is defined as the time taken for an investment to pay itself out, i.e., the amount of time it takes for the investor to gain back what it had invested. The return of investment period can be obtained by evaluating the  $n$  variable in the Net present Value (NPV) equation (30):

$$\Delta\text{profit} \cdot \sum_{t=1}^n \frac{1}{(1+i)^t} - U > 0 \quad (30)$$

Where  $n$  is the total time taken by the above relation to be true and  $i$  is the interest ratio.

In this case the initial investment would be the P.E.S unit and the needed connection. The cost of the unit is 2000 €<sup>6</sup>, while the cost of the connection can also be ignored.

Assessing profit is more difficult since is dependent on how the unit is applied.

Profit is defined as:  $\Delta\text{profit} = \Delta\text{revenue} - \Delta\text{costs}$ . Revenue and costs are balanced according to the company's goals.

---

<sup>6</sup> The actual price of the unit was not available, it was done an estimation by the sum of the cost of all components present in PESU plus a certain profit.

Revenues are directly proportional to productivity. Productivity is dependent on the station with the longest time cycle. If the unit is mounted on the station with the longest time cycle, or if the station where the unit is mounted becomes the station with the longest time cycle, productivity will decrease. Total revenue will probably decrease as well. The unit also saves energy, total cost will decrease as well. But according to the application, profit may decrease or increase. then:

$$\begin{aligned} \Delta \text{revenue} &= \Delta \text{ total production value} \\ &= \Delta \text{produce products} \cdot \text{product value} \end{aligned} \quad (31)$$

$$\Delta \text{costs} = \Delta \text{amount of used CA} \cdot \text{average cost of CA} \quad (32)$$

If instead, the unit is mounted to a station where the increase of time cycle won't affect production. Costs will decrease due to the lower amount of C.A. used. Profit will certainly increase.

By assuming:

- PESU is applied to one station
- the average cost of CA=0.044 €/kg (double of what reported in (6))
- interest  $i=8\%$  (latest inflation value recorded in Italy)
- $\Delta \text{amount of used CA} = (-1 + \text{GAIN}_{(\text{air consumption})}) \cdot \dot{m}_{(\text{no PESU})} \cdot \text{TOT}_{\text{time}}$
- $\Delta \text{produce products} = 1 - \text{GAIN}_{(\text{cycle time consumption})}$
- $\dot{m}_{(\text{no PESU})} = 0.483 \text{ kg/min}$  from test 2<sup>7</sup>
- $\text{TOT}_{\text{time}} = 8$  full shift hour for 252 working day a year

Daily the total amount of costs saving is about 3.98 €. Even if the application of PESU in a production plant would cause even a small delay, it would not be fruitful investment.

On the other hand, if the unit does not influence total revenue,  $\Delta \text{revenue} = 0$ , then PESU has a return of investment of 3 years. Calculations were done by just considering reduction in energy consumption to produce CA. It must be reminded that a reduction in compressed air production implies in a longer life of compressor and of other pneumatic components.

---

<sup>7</sup> Value obtained by dividing the total amount of CA used in test 2 (calculated as showed in chapter 6.3) divided by the time of the experiment (which is 2 minutes in all the experiments)

## **10 Conclusion**

These experiments were done to evaluate the effects of PESU in pneumatic system. First a pneumatic system was developed. It was also briefly explained on how the systems and their component worked.

PESU was found to reduce overall CA consumption to complete the same operation. It also was found that PESU generates back-pressure, which for reason explained in the previous chapters, reduces the actuator's speed.

### **10.1 PESU speed reduction**

From an economic point of view actuators' speed reduction is not liable. Production rate must be always kept at maximum speed. By reducing back-pressure actuators' speed will increase and be brought even to higher value than in the case where PESU is not used.

### **10.2 Possible future tests**

A way to reduce back pressure can be to install quick exhaust valve at the actuator exhaust. This way the exhaust flow rate will experience the pressure drop given by the quick exhaust valve and not by DCV (DCV pressure drop is usually high). Unfortunately, no test was done with this set up.

Additional experiments may consist in testing PESU for longer than two minutes. This would help on analyzing the system behaves when PESU is applied: if temperature increase is significant or not, or how it behaves if maximum tank pressure drop is smaller than 0.2 bar, as recorded in paragraph 8.6 .

Additionally, the system can be studied with a compressor acting as the only external supply. This way the system could be tested with known input power values.

### **10.3 Economic liability of PESU**

A small economic analysis was done. PESU is a relative cheap component, it is easy to install and does not require continuous setting. Results from the economic analysis showed that PESU energy saving capacity is not of great economic importance. This is mainly due to the low costs of pneumatic energy. Neither the less, due to its low costs, PESU can return its investment in a less than 3 years if its application does not lower productivity.

With the collected data, PESU is a liable investment only when its application does not involve a reduction in productivity.

## **10.4 Issue with gathered data**

Collected data are sufficient for a brief evaluation of PESU in a CAS. Data are not rigorous. First pressure values were collected outside the actuator chamber. This pressure values, even though they are shown to be consistent with mass flow rates values (chapter 6.3), do not represent, at some time instant, the actual pressure values in the actuator. This is the case of the issue with the cushioning system present in actuator 1 described in chapter 8.2.

## 11 Bibliography

1. Steen M. GREENHOUSE GAS EMISSIONS FROM FOSSIL FUEL FIRED POWER GENERATION SYSTEMS. :61.
2. Hernandez-Herrera H, Silva J, Diaz V, Sanchez Z, García G, Escorcía S, et al. Energy Savings Measures in Compressed Air Systems. *Int J Energy Econ Policy*. 2020 Mar 15;10:414–22.
3. Hingorani A, Pavlov A. Energy Efficiency in Compressed Air Systems. 2010 [cited 2022 Apr 12]; Available from: <https://oaktrust.library.tamu.edu/handle/1969.1/94051>
4. Love LJ. Estimating the Impact (Energy, Emissions and Economics) of the US Fluid Power Industry [Internet]. 2012 Dec [cited 2022 Apr 12] p. ORNL/TM-2011/14, 1061537. Report No.: ORNL/TM-2011/14, 1061537. Available from: <http://www.osti.gov/servlets/purl/1061537/>
5. Bonfá F, Benedetti M, Ubertini S, Introna V, Santolamazza A. New efficiency opportunities arising from intelligent real time control tools applications: the case of Compressed Air Systems' energy efficiency in production and use. *Energy Procedia*. 2019 Feb;158:4198–203.
6. Abela K, Francalanza E, Refalo P. Utilisation of a compressed air test bed to assess the effects of pneumatic parameters on energy consumption. *Procedia CIRP*. 2020;90:498–503.
7. Kosturkov RD, Nachev VG, Titova TP. Expert estimation of leakage losses in the pneumatic systems in the

- bottling industry. IOP Conf Ser Mater Sci Eng. 2020 Jun 1;878(1):012008.
8. Billep J, Fleischhacker H. Reduce energy costs in compressed air systems by up to 60%. *Asset Manag Maint J.* 29(3):41–6.
  9. Seslija D, Milenkovic I, Dudic S, Sulc J. Improving energy efficiency in compressed air systems - practical experiences. *Therm Sci.* 2016;20(suppl. 2):355–70.
  10. Blagojević V, Šešlija D, Stojiljković M, Dudić S. Efficient control of servo pneumatic actuator system utilizing by-pass valve and digital sliding mode. *Sadhana* [Internet]. 2013 May 4 [cited 2022 Apr 19]; Available from: <http://link.springer.com/10.1007/s12046-013-0131-7>
  11. Blagojevic V, Seslija D, Dudic S, Randjelovic S. Energy Efficiency of Pneumatic Cylinder Control with Different Levels of Compressed Air Pressure and Clamping Cartridge. *Energies.* 2020 Jul 19;13(14):3711.
  12. Cummins JJ, Nash CJ, Thomas S, Justice A, Mahadevan S, Adams DE, et al. Energy conservation in industrial pneumatics: A state model for predicting energetic savings using a novel pneumatic strain energy accumulator. *Appl Energy.* 2017 Jul;198:239–49.
  13. US9765786booster\_patent.pdf.
  14. vba.pdf [Internet]. [cited 2022 Jun 21]. Available from: <https://www.smc-pneumatics.com/pdfs/vba.pdf>
  15. Käyttöohje.pdf.

16. Michael J. Moran, Howard N. Shapiro, Bruce R. Munson, David P. DeWitt. Introduction to Thermal Systems Engineering: Thermodynamics, Fluid Mechanics, and Heat Transfer. John Wiley & Sons, Inc.; 2003. 59–89 p.
17. Should You Lubricate Your Pneumatic System? | SMC Corporation of America [Internet]. [cited 2022 Jun 11]. Available from: <https://www.smcusa.com/help-support/best-practices/should-you-lubricate-your-pneumatic-system/>
18. PFMC catalogue.pdf.
19. MATLAB Toolboxes [Internet]. Tamas Kis. [cited 2022 Jun 13]. Available from: <https://tamaskis.github.io/>
20. VXZ2-A\_EU.pdf [Internet]. [cited 2022 Jul 25]. Available from: [https://static.smc.eu/pdf/VXZ2-A\\_EU.pdf](https://static.smc.eu/pdf/VXZ2-A_EU.pdf)
21. British Standards Institution, British Standards Institution. Method for determination of flow-rate characteristics of pneumatic fluid power components. London: British Standards Institution; 1990.
22. Pneumatic Flow-rate Characteristics / Composite Calculation / Search Software - SMC Corporation [Internet]. [cited 2022 Jun 17]. Available from: <https://mssc.smcworld.com/fccs/#/item-select>
23. IQAN\_catalog\_HY33-1800\_us.pdf [Internet]. [cited 2022 Jun 15]. Available from: <https://www.parker.com/Literature/Electronic%20Cont>

rols%20Division/Literature%20files/IQAN\_catalog\_HY  
33-1800\_us.pdf

## Appendix A

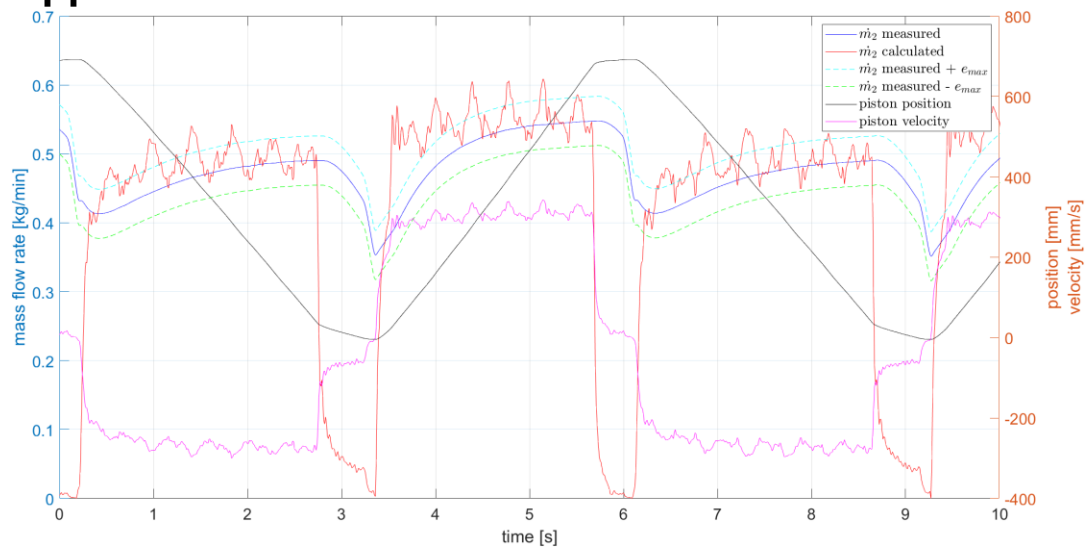


Figure 42: comparing mass flow rate 2 from sensor readings to the calculated from piston's velocity.

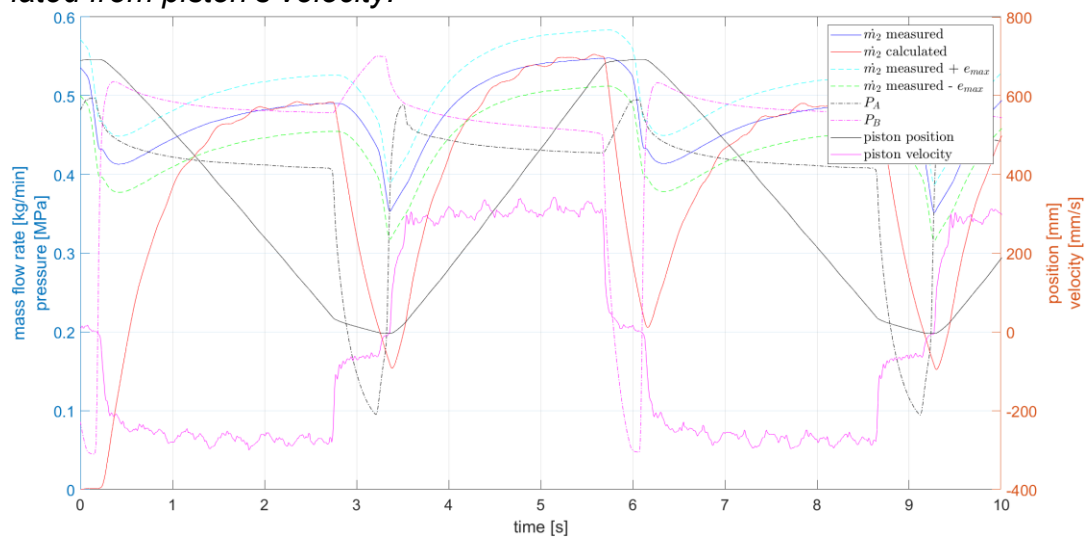


Figure 43: values reported in Figure 42 with sensor dynamics

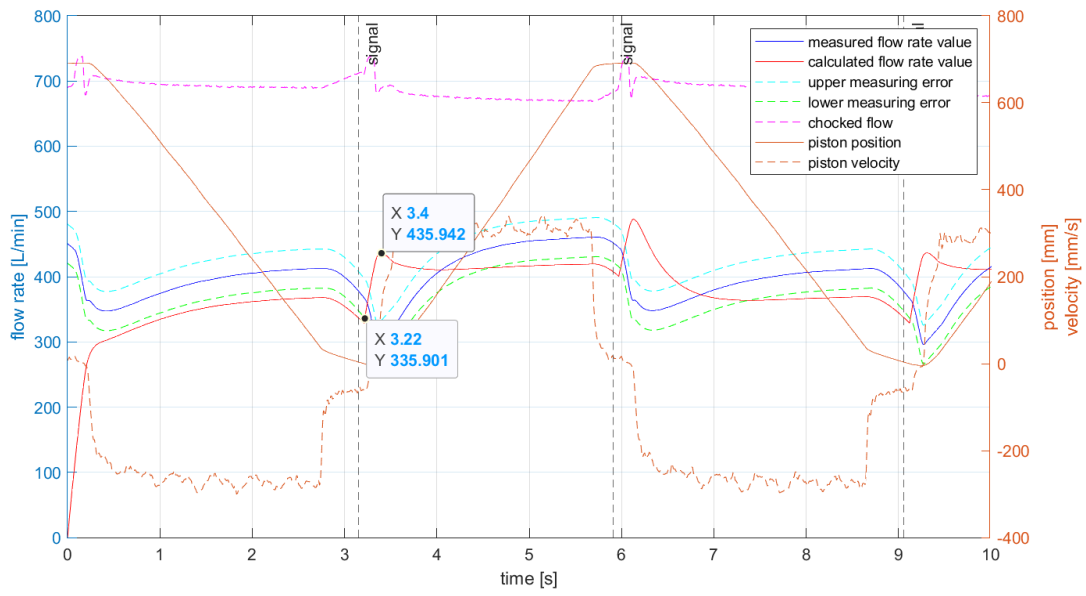


Figure 44: delay in transient.

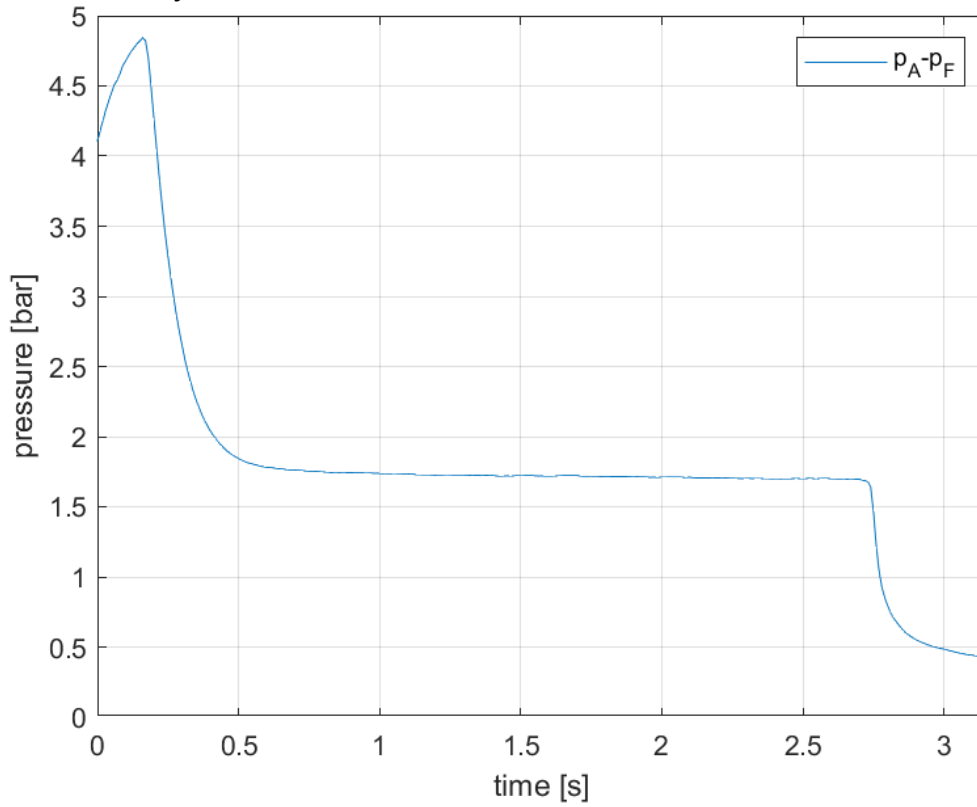


Figure 45: exhaust flow rate pressure difference.

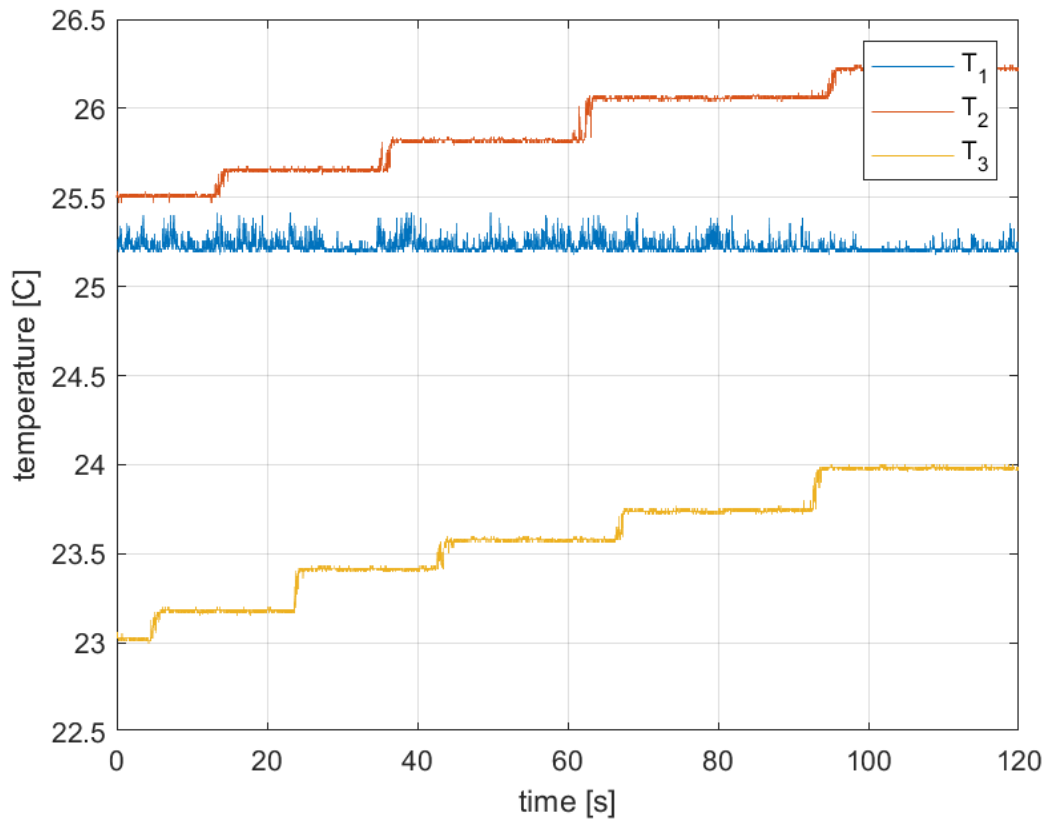


Figure 46: temperature difference test 1.

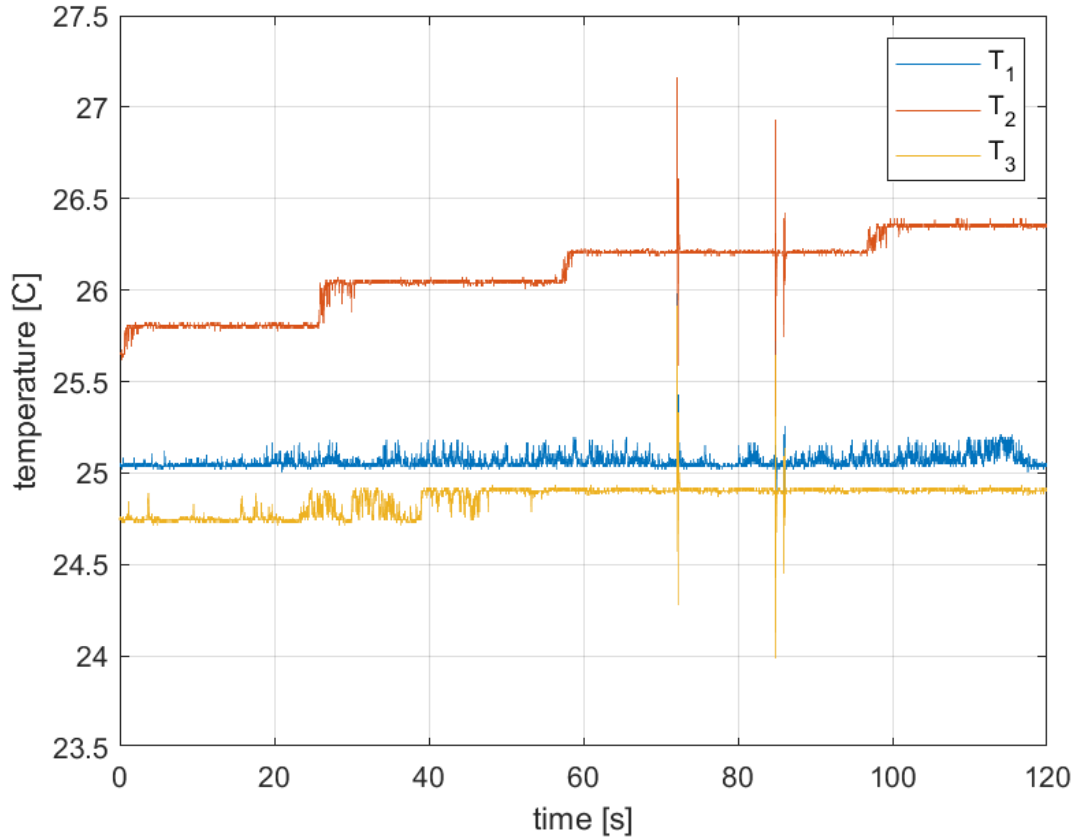


Figure 47: temperature difference test 2.

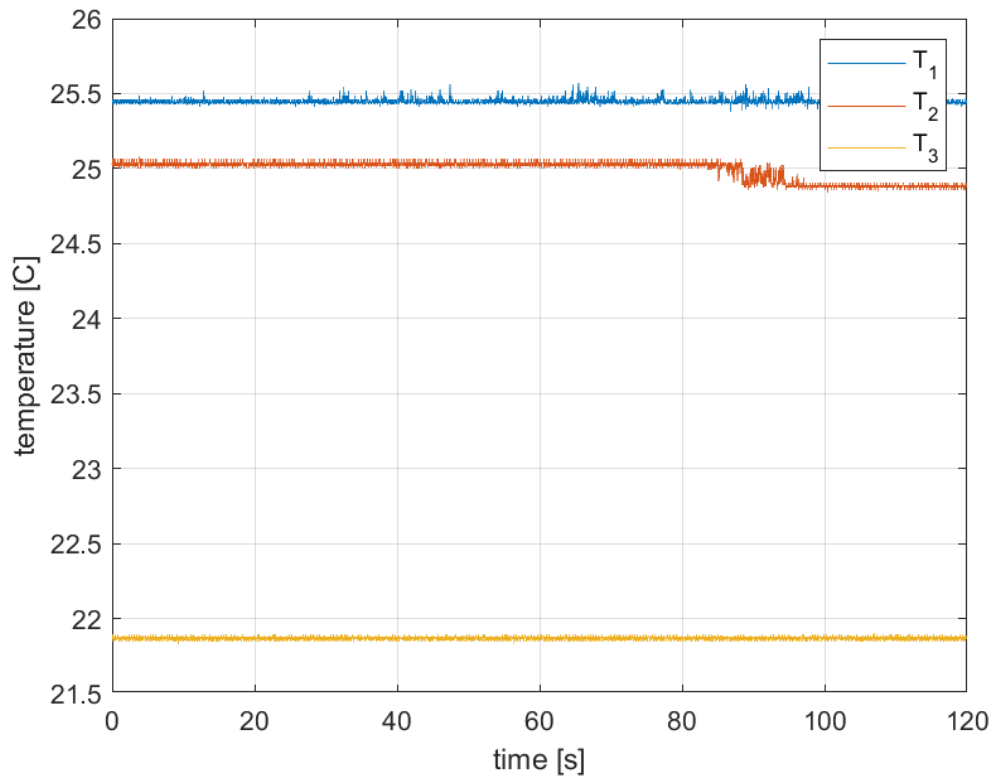


Figure 48: temperature difference test 3.